Quantifying the relative contributions of riparian and hillslope zones to catchment runoff

Brian L. McGlynn

Department of Land Resources and Environmental Sciences, Montana State University, Bozeman, Montana, USA

Jeffrey J. McDonnell

Department of Forest Engineering, Oregon State University, Corvallis, Oregon, USA

Received 24 February 2003; revised 2 June 2003; accepted 26 August 2003; published 6 November 2003.

[1] The spatial and temporal sources of headwater catchment runoff are poorly understood. We quantified the contributions of hillslopes and riparian zones to streamflow for two storm events in a highly responsive, steep, wet watershed located on the west coast of the South Island of New Zealand. We examined the spatial and temporal components of catchment storm flow using a simple continuity-based approach. We tested this with independent isotopic/solute mass balance hydrograph separation techniques. We monitored catchment runoff, internal hydrological response, isotopic, and solute dynamics at a trenched hillslope, and at hillslope and riparian positions in a 2.6-ha catchment. The gauged hillslope was used to isolate and quantify (by difference) riparian and hillslope zone contributions to the 2.6-ha headwater catchment. Utilizing flow-based approaches and a tracer-based mass balance mixing model, we found that hillslope runoff comprised 2–16% of total catchment storm runoff during a small 27-mm event and 47–55% during a larger 70-mm event. However, less than 4% of the new water collected at the catchment outlet originated from the hillslopes during each event. We found that in the 27-mm rain event, 84–97% of total storm runoff was generated in the riparian zone. In a larger 70-mm event, riparian water dominated total flow early in the event, although the hillslope became the main contributor once hillslope runoff was initiated. Despite the large amount of subsurface hillslope runoff in total storm runoff during the second larger event, riparian and channel zones accounted for 96% of the new water measured at the catchment outlet. Riparian water dominated between events, throughout small runoff events, and during early portions of large events. While this sequencing of catchment position contributions to flow has been conceptualized for some time, this is the first study to quantify this timing, constrained by hydrometric, isotopic, and solute approaches. *INDEX TERMS:* 1860 Hydrology: Runoff and streamflow; 1836 Hydrology: Hydrologic budget (1655); 1806 Hydrology: Chemistry of fresh water; 1829 Hydrology: Groundwater hydrology; 1866 Hydrology: Soil moisture; *KEYWORDS:* riparian zone, hillslope, hydrograph separation, mixing models, buffer zones

Citation: McGlynn, B. L., and J. J. McDonnell, Quantifying the relative contributions of riparian and hillslope zones to catchment runoff, *Water Resour. Res.*, *39*(11), 1310, doi:10.1029/2003WR002091, 2003.

1. Introduction

[2] The catchment landscape units controlling storm runoff generation, its timing, and mixing dynamics are poorly understood. While the geographic sources [*Hooper and Shoemaker*, 1986; *Bazemore et al.*, 1994; *Hinton et al.*, 1994; *Scanlon et al.*, 2001] and temporal sources [*Sklash et al.*, 1986; *Pearce et al.*, 1986; *McDonnell*, 1990; *Burns et al.*, 2001] of storm flow have been widely studied, a generalizable understanding of which landscape units contribute to which parts of the storm hydrograph remains elusive. This is important because until we can relate catchment position cause to stream effect, models of land use change, nonpoint source pollution, and the like will be poorly constrained. To date, researchers have been forced to infer where in the catchment runoff originates based on solute or isotopic data collected at the catchment outlet, sometimes with the aid of a handful of internal point measurements. This is problematic because different flow paths and combinations of source waters can exhibit similar isotopic, hydrochemical, or local hydrological responses [*Kendall et al.*, 2001]. As a consequence of this, widely applicable catchment models and hydrological scaling relationships have been difficult to determine. This equifinality, where multiple combinations of sources, flow paths, internal hydrological dynamics, and runoff mechanisms can result in the same signal as measured at the catchment outlet, is a major impediment to further progress in understanding where water goes when it rains and what flow path it takes to the stream.

[3] We have known for some time that hillslopes and near-stream riparian zones behave and respond differently

0043-1397/03/2003WR002091

to storm rainfall. Indeed, early streamflow generation research of the International Hydrological Decade (IHD) [e.g., *Whipkey*, 1965; *Hewlett and Hibbert*, 1967; *Ragan*, 1968; *Weyman*, 1970; *Dunne and Black*, 1970a, 1970b] has formed the core of our present-day hydrological understanding of how hillslopes and near-stream zones "work," based largely upon physical measurements of soil moisture, water table dynamics, and runoff. Processes such as infiltration excess overland flow [*Horton*, 1933], subsurface storm flow [*Hewlett and Hibbert*, 1963; *Whipkey*, 1965; *Kirby and Chorley*, 1967; *Weyman*, 1970], translatory flow [*Hewlett and Hibbert*, 1967] on hillslopes and return flow [*Dunne*, 1978], variable source area overland flow [*Hewlett and Hibbert*, 1967; *Dunne and Black*, 1970a, 1970b] on near-stream riparian zones have become well entrenched in the literature. While useful initially in helping to define different runoff processes in different environments, static process descriptions such as these have not proven useful in understanding the relative role of different landscape positions volumetrically and geochemically at the catchment outlet, how hillslope zones contribute to, displace, and/or mix with water in the valley bottom, and how the relative contributions of water from these different catchment units might affect the stream signal. These are fundamentally different questions from what we asked during the IHD when the focus was on storm flow amounts and how rapid runoff was delivered to the channel.

[4] Catchment hydrology has seen the methodological shift from IHD runoff volume focus to hydrograph-based tracer deconvolution approaches. Hydrograph separations of catchment runoff into old and new water have become widely accepted and have demonstrated that runoff is dominated typically by stored old water [*Pinder and Jones*, 1969; *Hooper and Shoemaker*, 1986; *Kennedy et al.*, 1986; *Rodhe*, 1987]. While two-component separations have given way to three-component separations based on two tracers [*Ogunkoya and Jenkins*, 1993; *Bazemore et al.*, 1994] and three-component multitracer separation approaches such as end-member mixing analysis [*Hooper et al.*, 1990; *Christopherson et al.*, 1990; *Christophersen and Hooper*, 1992], these approaches still do not resolve how water gets to the stream. Indeed the limitations of purely mixing-based analyses have been increasingly recognized [*Bonell*, 1998; *Rice and Hornberger*, 1998; *Genereux*, 1998]. These limitations range from difficulties in accurately characterizing and quantifying runoff source areas, to spatial and temporal variability in end-member compositions, to treating catchments as black boxes where a multitude of combinations of tracer concentrations and volumes in addition to flow paths and streamflow generation mechanisms may result in similar outflow tracer dynamics.

[5] Catchment hydrology seems stuck, in the sense that we have learned about as much as we can from single plots and reductionist study of specific runoff mechanisms, and we now know that most of the water in the channel during an event is water that existed in the watershed prior to the rainfall event. In this paper we argue for a new approach, one where we treat the most basic units of the watershed (in this case hillslopes and riparian zones) and examine how they store, receive, and deliver water during and between events. We present this work for the Maimai watershed in New Zealand, where the distinction between hillslopes and riparian zones is clear, landscape organization is relatively simple [*McGlynn and Seibert*, 2003], and we can build on a wealth of prior research [*McGlynn et al.*, 2002].

[6] Our focus on landscape controls on streamflow generation is not new. Indeed, several recent papers have examined ways to disaggregate the land surface into subareas of uniform "quasi-homogeneous" behavior [*Becker and Braun*, 1999] such as hydrological response units (HRUs) [*Wigmosta et al.*, 1994; *Leavesley and Stannard*, 1995; *Grayson et al.*, 1995] or dynamic contributing areas [*Beven and Freer*, 2001]. However, these studies to date have been based on a quest for improved model performance and not necessarily on a better process understanding of catchment runoff and solute export controls. Those studies that have done this from a process perspective [*Uhlenbrook*, 1999; *Sidle et al.*, 2000] have done so only qualitatively, without a formal "breaking up" of the landscape, literally and figuratively.

[7] We postulate that combinations of techniques utilizing extensive survey, hydrometric, isotopic, and solute data in a landscape discretization context are necessary to obtain an unequivocal understanding and quantification of both spatial and temporal runoff sources. In this way, we seek to ascertain the fundamental landscape controls on small catchment runoff generation. We measure at the scale at which we want to understand, specifically, dominant landscape units in headwater catchments (hillslope zones and riparian zones) to address the following questions: (1) Where does new water observed at the catchment outlet originate? (2) What are the relative proportions of hillslope and riparian zone sources of catchment runoff? (3) Does solute and isotopic evidence support hydrometric based runoff source estimations? (4) How does the riparian zone modulate hillslope inputs to the stream?

[8] Building upon a wealth of prior research at the Maimai catchments (see review by *McGlynn et al.* [2002]) related to the evolution of a detailed perceptual model of hillslope hydrology, the research outlined in this paper serves to quantify the relative roles of hillslopes and riparian zone runoff generation. We seek to understand the dominant controls on catchment runoff by breaking the catchment into discrete landscape units. We then apply a simple hydrometric mass balance separation model and test the hydrometric model with tracer-based mass balance modeling approaches. Through these combined techniques, we seek to quantify basic catchment behavior that motivated the early studies of the International Hydrological Decade, this time heeding *Bonell*'s [1998] call for providing a formal framework for hydrological units and their interaction.

2. Study Site

[9] This study was conducted at the Maimai research catchments located on the west coast of the South Island of New Zealand (Figure 1a). Maimai is a benchmark hydrological research site with a long history of hydrological and ecological research. *McGlynn et al.* [2002] provide a review of hydrological research at Maimai. The Maimai research area consists of multiple catchments that form the headwaters of the Grey River, located to the east of the Paparoa Mountain range. Slopes are short (<300 m), steep

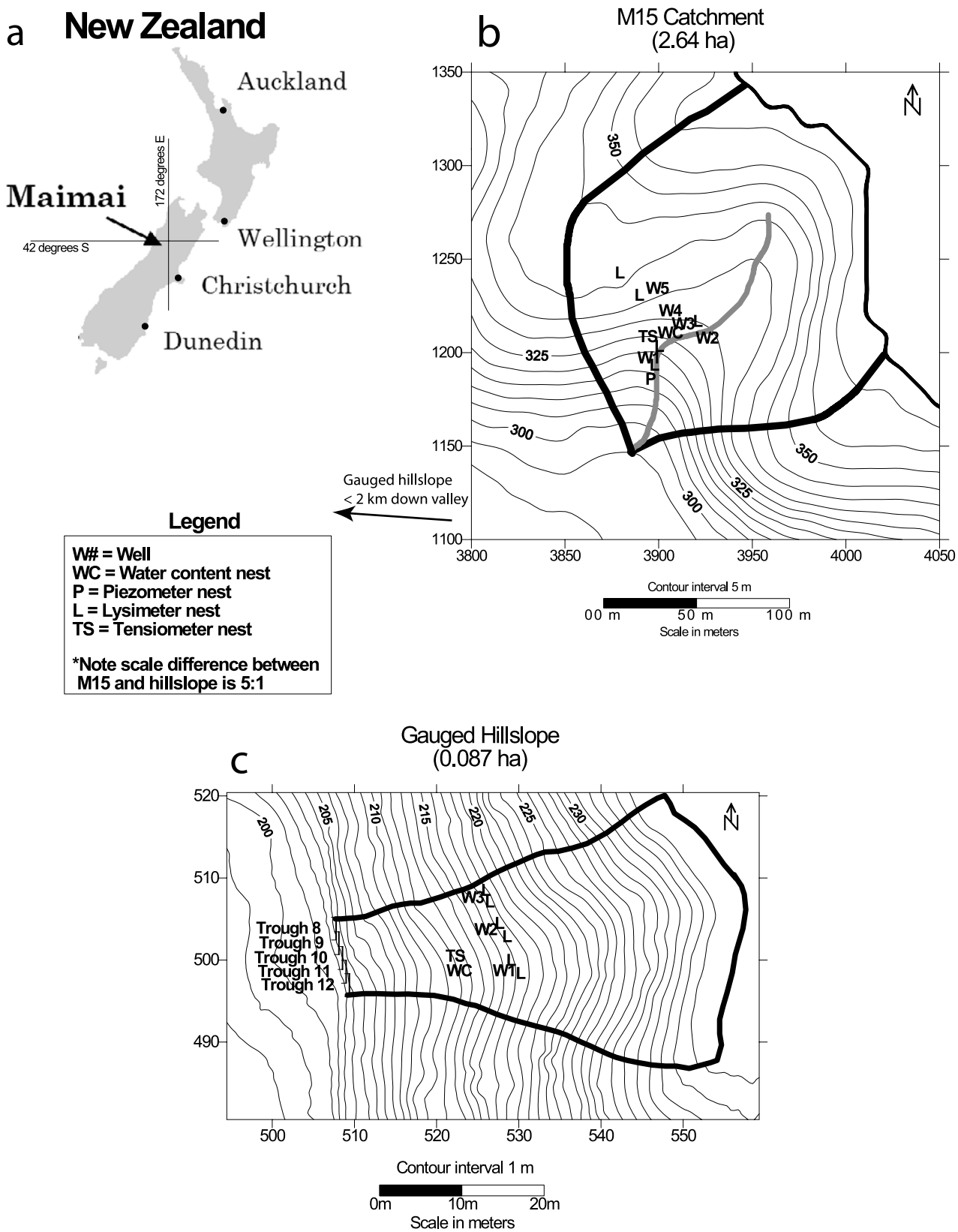

Figure 1. (a) Location of study area on the west coast of the South Island of New Zealand. (b) Detailed map of topography and instrumentation locations in the M15 catchment. (c) Detailed map of topography and instrumentation locations on the gauged hillslope.

(average 34°), and have local relief ranging from 100 to 150 m. Much of the hydrological research to date has been directed toward adjacent, remarkably similar, catchments ranging in size from 1.6 to 8 ha, sharing similar topographic, geologic, and soil characteristics [*Pearce et al.*, 1976; *Mosley*, 1979, 1982; *Pearce et al.*, 1986; *Sklash et al.*, 1986; *Moore*, 1989; *Rowe et al.*, 1994]. The research described in this paper was conducted within the Maimai M15 catchment (2.6 ha) and at a nearby (<2 km down valley) excavated and trenched hillslope (0.087 ha) (Figure 1).

[10] Annual precipitation averages 2600 mm and produces approximately 1550 mm of runoff, and rainfall occurs on average 156 days per year [*Rowe et al.*, 1994]. The catchments are highly responsive to storm rainfall. Quickflow (QF, as defined by *Hewlett and Hibbert* [1967]) comprises 65% of the mean annual runoff and 39% of annual total rainfall (P) [*Pearce et al.*, 1986]. *Pearce et al.* [1986] note that the R index for QF/P averaged for runoff events from rainfalls of greater than 25 mm is 46%, compared with 3–35% for 11 basins distributed between Georgia and New Hampshire [*Hewlett and Moore*, 1976].

[11] The vegetation in the M15 catchment is mixed evergreen beech (*Nothofagus* spp.), podocarps, and broadleafed hardwoods. It is multistoried, with a canopy 20–36 m high, a dense fern and shrub understory, and a fern and moss ground cover. A firmly compacted, moderately weathered, early Pleistocene conglomerate, known as the Old Man Gravels, underlies the Maimai catchments. The conglomerate is composed of clasts of sandstone, granite, and schist in a tight clay-sand matrix and is nearly impermeable, with estimates of seepage losses to deep groundwater of only 100 mm/yr [*O'Loughlin et al.*, 1978; *Pearce and Rowe*, 1979]. Soils overlying the Old Man Gravels are classified as Blackball Hill soils. Silt loam textures predominate. Typical soil profiles are characterized by thick, well-developed organic horizons (average 17 cm), thin, slightly stony, dark grayish brown A horizons, and moderately thick, very friable mineral layers of podsolized, stony, yellow-brown earth subsoils (average 60 cm). Study profiles examined by *Webster* [1977] showed mean total porosity and macroporosity of 86% and 39% by volume and an infiltration rate of 6100 mm/h for the organic humus layer. The mineral soils are permeable and promote rapid translocation of materials in suspension or solution [*Rowe et al.*, 1994]. The total profile porosity averaged 70% by volume, bulk densities averaged 0.80 t/m^3, and saturated hydraulic conductivities averaged 250 mm/h. The soils remain within 10% of saturation by volume during much of the year due to the wet environment. As a result, the soils are strongly weathered and leached and have low natural fertility [*Mosley*, 1979].

[12] *Mosley* [1979, 1982] found that soil profiles at vertical pit faces in the Maimai M8 catchment revealed extensive macropores and preferential flow pathways which formed along cracks and holes in the soil and along live and dead root channels. Soil pits excavated in the M15 catchment and on the gauged hillslope used in this study were comparable and corroborated Mosley's observations. Preferential flow was observed regularly along soil horizon planes and along the soil-bedrock (Old Man Gravels) interface in this study and in historical research [*Mosley*, 1979, 1982; *McDonnell*, 1990; *Woods and Rowe*, 1996; *Brammer*, 1996; *McDonnell et al.*, 1998; *McGlynn et al.*, 2002].

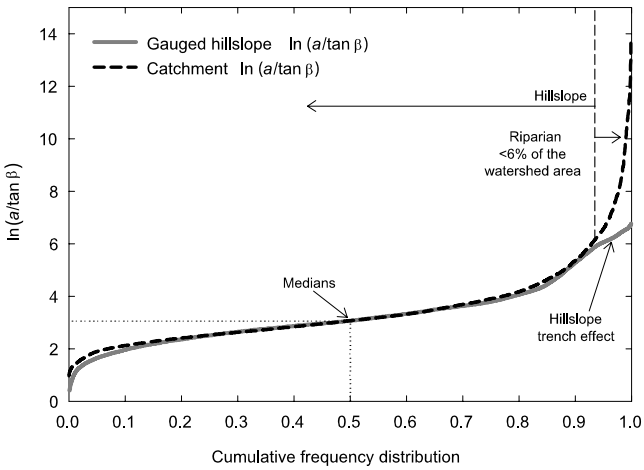

Figure 2. The gauged hillslope and hillslopes comprising a Maimai headwater catchment show comparable distributions of the topographic index ln a/tanβ (mean 3.5 versus 3.2, 5% trimmed mean 3.3 versus 3.2 median 3.1 versus 3.0). The vertical dashed line denotes <6% of the catchment area; the >94% of the catchment cumulative frequency distribution toward the origin represents hillslopes and the <6% to the right represents riparian areas and strongly convergent hollows not found on the gauged hillslope.

3. Methods

3.1. Hillslope Zone Instrumentation

[13] We reactivated the hillslope trench (located in the M8 catchment) excavated by *Woods and Rowe* [1996]. A subset of the original trench (troughs T8–T12) was instrumented and gauged at 5-min intervals (Figure 1c). Runoff from each 1.7-m trench section was collected in gutters sealed to the bedrock surface at the trench face and measured with 1-L tipping buckets (see *Woods and Rowe* [1996] for a detailed description). Flow proportional sampling of hillslope runoff was accomplished by subsampling (diverting) 6 mL from each 1-L bucket tip from high-flow trough T11 and low-flow trough T8. Subsampled flow was routed downslope to sequential samplers outfitted with ten 1.5-L collection bottles. Sequential samples typically represented 250 tips. Calibration checks of sequential samplers were made through each event. The time period associated with each sequential sample was flow rate dependent and determined based on the number of tips recorded and the number of sequential sample bottles filled. The sequential sampler design is conceptually similar to sequential rainfall sampler designs.

[14] Ten meters upslope of the hillslope trench face, in the central axis of the hillslope hollow above trough T11, nests of Campbell CS-615 water content probes and tensiometers were installed. Water content probes and tensiometers were located at three depths (0.3, 0.6, and 1 m), and recorded at 5-min intervals (Figure 2). Three fully screened 90-mm groundwater wells, instrumented with recording capacitance rods (Tru Track, Inc., model WTDL 8000), were completed to the soil-bedrock boundary (0.5–1.75 m) at locations

upslope of troughs T11 (well 1), T10 (well 2), and T8 (well 3). Water table depth was recorded at 5-min intervals. Wells were sampled during precipitation events for solute and isotopic analysis by stage-activated in situ samplers as the water table rose and manually sampled with a peristaltic pump as water tables receded. Three nests of 57-mm porous cup suction lysimeters evacuated to −35 kPa were completed in pairs: one at the A/B horizon boundary and the second near the base of the soil profile. Lysimeters were installed 15 m upslope of troughs T12, T11, and T8 and sampled prior to, during, and following precipitation events.

3.2. M15 Catchment Instrumentation

[15] The Maimai M15 catchment (2.6 ha) was instrumented with seven 90-mm diameter recording wells, a nest of recording piezometers, a nest of three recording Campbell CS-615 water content probes (0.1, 0.3, and 0.5 m depths), a colocated nest of three recording tensiometers, and three nests of 57-mm porous cup suction lysimeters. Data from recording instrumentation were collected at 5-min intervals, and isotopic and chemistry samples were collected from wells with stage activated in situ samplers as the water table rose and then manually sampled with a peristaltic pump as water tables receded. Suction lysimeters were evacuated to −35 kPa, and isotope and chemistry samples were collected from them prior to, during, and following precipitation events. Instrumentation was located primarily in riparian and lower hillslope positions; however, two wells were located in midslope positions for corroboration of the instrumented and trenched hillslope response. Streamflow was computed at 5-min intervals from stream stage measured at the M15 catchment outlet with a 90° V-notch weir and a capacitance rod. Rainfall was measured in 0.2-mm increments with a tipping bucket rain gauge located at the base of the excavated and trenched hillslope. Precipitation samples were collected in 5-mm increments with a sequential rainfall sampler and analyzed for $\delta^{18}O$, major cations, and silica.

[16] Samples for chemical and isotopic analysis were collected in 250-mL high-density polyethylene bottles. Subsamples for chemical analysis were passed through 0.45-μm glass fiber syringe filters. Cation samples were acidified to a pH of 1.0–1.5 with HCl prior to analysis for Ca^{2+}, Mg^{2+}, Na^{+}, K^{+}, and H_4SiO_4 concentrations by direct-coupled plasma emission spectroscopy. Analytical precision for H_4SiO_4 was 0.8 μmol/L. An unfiltered aliquot was subsampled for $\delta^{18}O$ analysis at the U.S. Geological Survey Stable Isotope Laboratory in Menlo Park, California, by mass spectrometer and reported in ‰ relative to Vienna standard mean ocean water (VSMOW) with 0.05‰ precision.

4. Modeling Methods

[17] In this paper we use the following definitions for temporal and spatial sources of catchment runoff: For temporal sources, "new water" is rainfall associated with the current storm event and "old water" is resident catchment water prior to the current storm event. For spatial sources, "hillslope water" is water originating from hillslope zones (old and new) and "riparian water" is water originating from riparian zones (old and new).

[18] We applied a simple flow-based hydrograph separation technique and used tracer-based mass balance models to constrain the spatial and temporal sources contributing to streamflow and test our flow-based model. The spatial (hillslope and riparian) sources of streamflow were first quantified with hydrological analysis and runoff separation based purely on observed hydrology. We then analyzed our results with a two-component isotopic hydrograph separation (old/new water) technique to quantify the amounts of new and old water generated in hillslope and riparian zones by both a small 27-mm and larger 70-mm storm event. We subsequently tested our results with three-component mass balance separations (old hillslope, old riparian, and new water) based on two tracers (silica and $\delta^{18}O$) to separate streamflow into its geographic and temporal sources. Initial flow-based analysis and subsequent multiple model validation approaches using tracer-based hydrograph separation/mixing models allowed for quantification of spatial and temporal runoff sources and insight into sequencing of runoff sources through events. In this paper we use the following definitions for each model: (1) Flow-based separation (FBS) is the flow-based mass balance hydrograph separation model; (2) two-component (2-CompHS) is the two-component one-tracer ($\delta^{18}O$) based mass balance hydrograph separation model (new and old water components); (3) three-component (3-CompHS) is the three-component two-tracer (Si and $\delta^{18}O$) based mass balance hydrograph separation model (old hillslope, old riparian, new components); and (4) three-component variable hillslope (3-CompVS) is the three-component two-tracer (Si and $\delta^{18}O$) based mass balance hydrograph separation model using a variable signature (hillslope) end-member composition (old hillslope, old riparian, new components).

4.1. Flow-Based Hydrograph Separation (FBS): Hillslope and Riparian Sources

[19] The gauged hillslope runoff dynamics, isotopic and solute signatures, and internal hillslope response to precipitation were consistent with those observed in hillslope positions in the M15 catchment. In addition, landscape analysis results demonstrated that the gauged hillslope was not unique, but rather was topographically comparable to hillslopes in the Maimai headwater catchments. We applied the area-normalized runoff monitored at the gauged hillslope to the entire hillslope area in the M15 catchment to determine the hillslope proportion of total M15 catchment runoff. This approach assumes that the gauged hillslope was characteristic of all the hillslopes in the M15 catchment or that it adequately represented the response of M15 hillslopes. We test this assumption with topographical, hydrological, isotopic, and solute analysis in subsequent sections. Furthermore, this assumption is implicitly tested in our approach: We test the flow-based separation model with independent solute-based mixing models. We assumed no time lag between hillslope runoff and catchment runoff because the hillslope trench was located at the base of the hillslope and thus assumed to be closely connected to catchment runoff timing. The difference between runoff observed at the catchment outlet and that derived from hillslope runoff estimates was then attributed to nonhillslope runoff (riparian runoff).

4.2. Multicomponent Hydrograph Separation

[20] Runoff from the M15 catchment and the gauged hillslope was separated into new and old water components

based on traditional two-component hydrograph separation methods (reviewed recently by *Buttle and McDonnell* [2003]). The rainfall or new water component was weighted based on the incremental mean weighting method as outlined by *McDonnell et al.* [1990] for each monitored event. For three sources contributing to streamflow (i.e., old hillslope, old riparian, and new water) the proportions of each component were determined using the standard [*DeWalle et al.*, 1988] approach. Where two tracers such as $\delta^{18}O$ and silica were used concurrently, the now-standard approach *Ogunkoya and Jenkins* [1993] was used to solve for three unknowns using two tracers simultaneously. Here again, the rainfall or new water component was weighted (for each monitored event) based on the incremental mean method of *McDonnell et al.* [1990]. Of course, unique source signatures are necessary for valid three-component hydrograph separations. Spatially and temporally constant source signatures are implicit, unless addressed explicitly as with the incremental weighting of the new water source or incremental application of a variable end-member signature.

[21] We also introduced a variable hillslope signature into the standard three-component model for comparative purposes (3-CompVS). In this separation, rain was weighted with the incremental mean approach of *McDonnell et al.* [1990] because of the spatially distributed nature of precipitation and the unknown travel times to the catchment outlet. Hillslope runoff, alternatively, was measured at the base of the hillslope, travel times to the catchment outlet were assumed to be small relative to precipitation, and therefore no weighting was applied. At each time step, the hillslope end-member signature was that measured in hillslope runoff.

4.3. Uncertainty Estimation

[22] Uncertainty estimations for the hydrological hydrograph separation were arbitrarily estimated as a constant 10% of each runoff component to account for potential measurement error and error in catchment discretization. Uncertainty in the three-component tracer-based separations was also assessed. Absolute errors of double the analytical precision for ^{18}O (0.1‰) and silica (1.6 μmol/L) analyses were propagated through the hydrograph separation equations based on the procedure outlined by *Genereux* [1998].

4.4. Method Integration

[23] Perhaps the greatest assumption of the flow-based hydrograph separation approach was that the gauged hillslope trench section provided an accurate representation of all hillslope units in the M15 catchment. Our research approach and study design have addressed this assumption directly. First, we tested the flow-based approach (FBS, based on gauged hillslope runoff) with the independent tracer-based model (3-compHS) and found strong agreement. In addition, we found strong agreement in isotopic and solute concentrations between gauged hillslope runoff and hillslope wells located in other catchments, including M15. Second, we compared the soil moisture and water table dynamics on the gauged hillslope with hillslope positions in the M15 catchment and other catchments in the larger Maimai watershed. On the basis of corroboration by over 12 months of concurrent gauged hillslope runoff and seven hillslope water table wells distributed across two Maimai headwater catchments (M15 and K), B. L. McGlynn et al. (The effects of catchment scale and landscape organization on streamflow generation, submitted to *Water Resources Research*, 2003; hereinafter referred to as submitted manuscript 2003) concluded that the gauged hillslope runoff dynamics adequately represented dynamics found in other monitored hillslope positions. Third, we compared topographic characteristics of the gauged hillslope to catchment wide hillslopes and found strong agreement for slope, soil depth, hillslope length, and distribution of the topographic index. Distributions of the topographic index $\ln a/\tan\beta$ were comparable (mean 3.47 versus 3.18, 5% trimmed mean (highest and lowest 5% of the ranked values discarded), 3.3 versus 3.16, and median 3.07 versus 3.02) between the M8 catchment and the gauged hillslope. Notwithstanding these corroborative tests, we acknowledge that there are soil depth and structure, slope angle and convergence, and potential vegetation variability among hillslopes that could result in a range of hillslope response characteristics. Therefore, in our analysis approach, we implicitly tested the gauged hillslope representativeness at the catchment scale by testing the hydrometric hydrograph separation results with tracer-based mixing models.

5. Results

5.1. Landscape Discretization

[24] Hillslopes and riparian zones often exhibit distinct hydrological characteristics due to their location in the landscape and very different combinations of local slope angle and upslope contributing area. Not surprisingly, our results showed that riparian zones respond (e.g., water tables develop or rise) more quickly to precipitation inputs than hillslope areas, as evidenced by data from wells, piezometers, tensiometers, and soil water content probes over 15 months of record (B. L. McGlynn et al., submitted manuscript, 2003). This difference is indicative of higher antecedent soil moisture and more persistent water tables in near stream positions. Hillslope positions drained more fully between events, resulting in higher between-storm soil moisture deficits. Our experimental design allowed us to highlight the difference between riparian and hillslope response early in storm events and throughout small events (<30 mm under dry antecedent conditions).

[25] The hillslope troughs provided measurements of hillslope runoff initiation, rates, and dynamics across a divergent-planar-convergent hillslope continuum. Typically, riparian zones exhibited soil characteristics reflecting higher average soil moisture status and prolonged periods of saturation. This results in soil gleying, the accumulation of fine sediments, and increased weathering and deposition. Because of the topographic, hydrologic, and pedologic variability between hillslope and riparian areas, clear, unambiguous differentiation and mapping based on solute signatures, soils, landform (topography), and response to storm precipitation were possible.

[26] The headwater Maimai catchments, including M15, are characterized by short steep slopes, abrupt breaks in slope, and narrow riparian zones. Headwater catchments that comprise the Maimai research area are remarkably similar in topographic, soils, and hydrologic characteristics [*McGlynn et al.*, 2002]. Hillslope and riparian areas are readily discerned and distinguished in the field based on landform, proximity to channel, slope, elevation, moisture status,

Table 1. Discretized Landscape Unit Areas, Volumes, and Ratios

Variable	M15 catchment
Catchment area[a]	26,400 m^2
Hillslope area	25,642 m^2
Channel area	183 m^2
Riparian area	575 m^2
Channel + riparian area	758 m^2
Hillslope/total catchment area	0.97
Riparian/total catchment area	0.02
(Riparian + channel)/catchment area	0.03
Hillslope volume[b]	15,385 m^3
Riparian volume	314 m^3
Riparian volume/hillslope volume	0.02

[a]Area refers to planar area.
[b]Volume refers to total soil reservoir and does not include porosity estimates.

hydrological response, and soil characteristics [*Webster*, 1977]. In the M15 catchment we mapped riparian areas and measured soil depths at transects (perpendicular to the stream channel) every 10 m or less from the catchment outlet to the point of channel initiation. Channel initiation typically occurred at accumulated area thresholds of 0.5 ha [*McGlynn and Seibert*, 2003]. We determined (conservatively) that the riparian area was 575 m^2 and the channel area was 183 m^2 (Table 1). Soil depths in the riparian areas ranged from 0.13 to 1 m and averaged 0.55 m. We determined hillslope area in the M15 catchment to be 25,642 m^2, computed as the difference between the mapped riparian area and the total catchment area. Mean soil depths for the hillslope areas were 0.6 m and ranged from 0.15 to 2 m (Table 2), as determined from detailed measurements across numerous <4-ha catchments by *Webster* [1977], at the gauged hillslope trench site by *Brammer* [1996], and corroborated with our soil depth surveys in the M15 catchment.

[27] The gauged hillslope was selected based on previous research results [*Woods and Rowe*, 1996; *Woods et al.*, 1997; *McDonnell et al.*, 1998; *McGlynn et al.*, 2002] and consisted of troughs T8–T12 that provided a cross section of hillslope characteristics typical of the M15 catchment, including discernable hollow, planar, and divergent slope sections. The gauged hillslope response and composition were comparable to hillslope water table response and solute characteristics monitored in other Maimai catchments as well as in the M15 catchment. We computed cumulative frequency distributions of the topographic index, $\ln a/\tan\beta$, where a is the upslope accumulated area and β is the local slope angle [*Beven and Kirkby*, 1979] for the gauged hillslope and the M8 catchment (Figure 2). The M8 catchment topographical survey was the only survey of sufficient resolution for comparison to our detailed gauged hillslope topographic survey. M8 topography has been described as remarkably similar to the other Maimai headwater catchments [*Pearce et al.*, 1986; *Mosley*, 1979; *Rowe et al.*, 1994; *McGlynn et al.*, 2002]. We found that the gauged hillslope $\ln a/\tan\beta$ distribution was comparable to the hillslopes in the Maimai catchment (M8) (Figure 2). The cumulative frequency distributions for the catchment and hillslope only diverge for high topographic index values associated with riparian areas and strongly convergent zero-order hollows that form <6% of the catchment area. Hillslope positions in the M8 catchment and the gauged hillslope are surprisingly similar in topographic index distribution, slope, and soil depth. Therefore the gauged hillslope topography is comparable to hillslopes across the catchments.

5.2. Hydrological Response

[28] We monitored two successive precipitation events over a 6-day period. Antecedent moisture conditions were low for event 1 (27 mm event on 14 May 1999), and significantly higher for event 2 (70 mm event on 16 May) that followed 36 hours later (Figure 3). The antecedent precipitation indices for event 1 were relatively low for the Maimai catchments, with API_{30} = 126 mm, API_{14} of 17 mm, and API_7 = 7 mm. Antecedent conditions for event 2 were greater, with an API_{30} = 122 mm, API_{14} of 44 mm, and an API_7 = 34 mm.

[29] Hillslope runoff exhibited a threshold response to precipitation as a result of dry antecedent conditions. Dry antecedent conditions were demonstrated by the negligible response to the first 40+ mm of precipitation associated with events 1 and 2 (Figure 3). Hillslope water content probes showed bypass flow to depth: progressive wetting of the shallow and deep portions of the soil profile with the midprofile soil moisture increasing slowly in response to precipitation. The water table in the gauged hillslope hollow lagged precipitation but water table rise was rapid once initiated. The soil profile moisture content and water table responded more quickly to event 2: Hillslope runoff was coincident with saturation development in the soil profile and water table rise in the bedrock depression. The bedrock depression is described by *McDonnell et al.* [1998] and *McGlynn et al.* [2002]. Significant hillslope runoff occurred only during event 2. However, event 2 response lagged 5 hours behind M15 catchment response, although hillslope peak runoff lagged M15 peak runoff by less than 1 hour. Area normalized hillslope runoff was 60% of M15 catchment runoff at peak flow (Figure 3d).

[30] A counterclockwise hysteretic relationship existed between hillslope runoff and M15 catchment runoff. Hillslope runoff was markedly lower on the rising limb of the M15 catchment hydrograph as compared to the same M15 catchment runoff on the falling limb (Figure 3d). On the rising limb, hillslope dynamics were disconnected from catchment runoff; however, on the falling limb of the hydrograph, a close linkage between hillslope runoff and catchment runoff was evident (i.e., greater hillslope proportion of total runoff). See results section on the relative timing of hillslope, riparian, and new water contributions to total runoff for more detailed discussion.

[31] Riparian water content response in the M15 catchment was rapid and showed progressive wetting front propagation through the soil profile from shallow to deep. The water table developed quickly in response to precipitation in both events 1 and 2 (Figure 4). The shallow soil water content closely mimicked catchment runoff response to both events. Riparian wells showed rapid water table rise

Table 2. M15 Catchment and Gauged Hillslope Characteristics

Site	Area	Soil Depth		Mean Slope
		Mean	Range	
Gauged hillslope	870 m^2	0.6 m	0.15–2 m	40%
M15 catchment	26,400 m^2	0.6 m	0–2 m	38%
M15 riparian zone	575 m^2	0.55 m	0.13–1 m	16.7% (streambed)

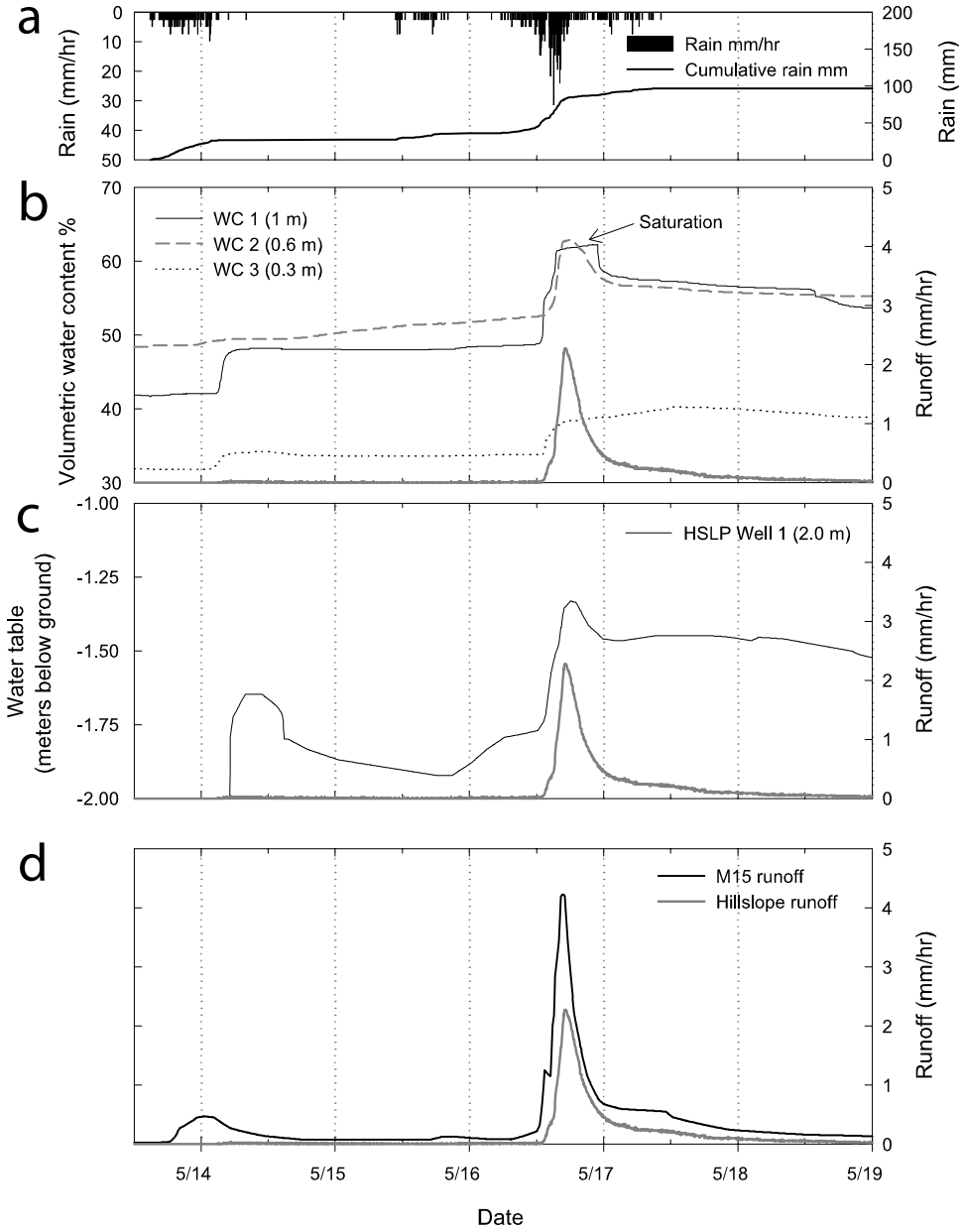

Figure 3. (a) Rainfall hyetograph and cumulative rain for event 1 (13–15 May 1999) and event 2 (15–18 May). (b) Gauged hillslope water content monitoring nest located 10 m upslope of trough 11. (c) Water table time series for hillslope well 1, located above trough 11 in a bedrock depression. (d) M15 catchment runoff and gauged hillslope runoff time series.

to the ground surface; water table response to precipitation was lagged and damped as distance from the channel increased (Figure 4). The M15 hillslope well 4 dynamics closely matched gauged hillslope runoff response, partially corroborating the representativeness of the gauged hillslope.

5.3. Flow-Based Hydrograph Separation

[32] The M15 runoff hydrograph was separated into runoff generated in hillslope zones and runoff generated in riparian zones. During event 1 (13 May 1200 LT to 15 May), 99% of M15 catchment runoff was generated in the riparian zone (Figure 5a, Table 3). It dominated runoff between events and formed all of the runoff during the initial 5 hours of runoff during the main event 2 hydrograph peak. Hillslope contributions were negligible and only occurred during the last third of event 1. Hillslope runoff remained minimal until 16 May at 1200 LT after 27 mm of rain associated with event 1 and 17 mm associated with event 2 had fallen. Once hillslope runoff was initiated, however, riparian water was rapidly displaced into the stream channel and hillslope water quickly formed the majority of catchment runoff. Hillslope runoff peaked less than 1 hour after catchment runoff. In event 2 (15 May to 19 May), riparian and hillslope runoff hydrographs were comparable in peak runoff rates (2.4–2.5 mm/hr) and volume (53–47% of total catchment runoff, respectively); however, they were distinct in their response timing to rainfall in both runoff initiation and recession. For the initial

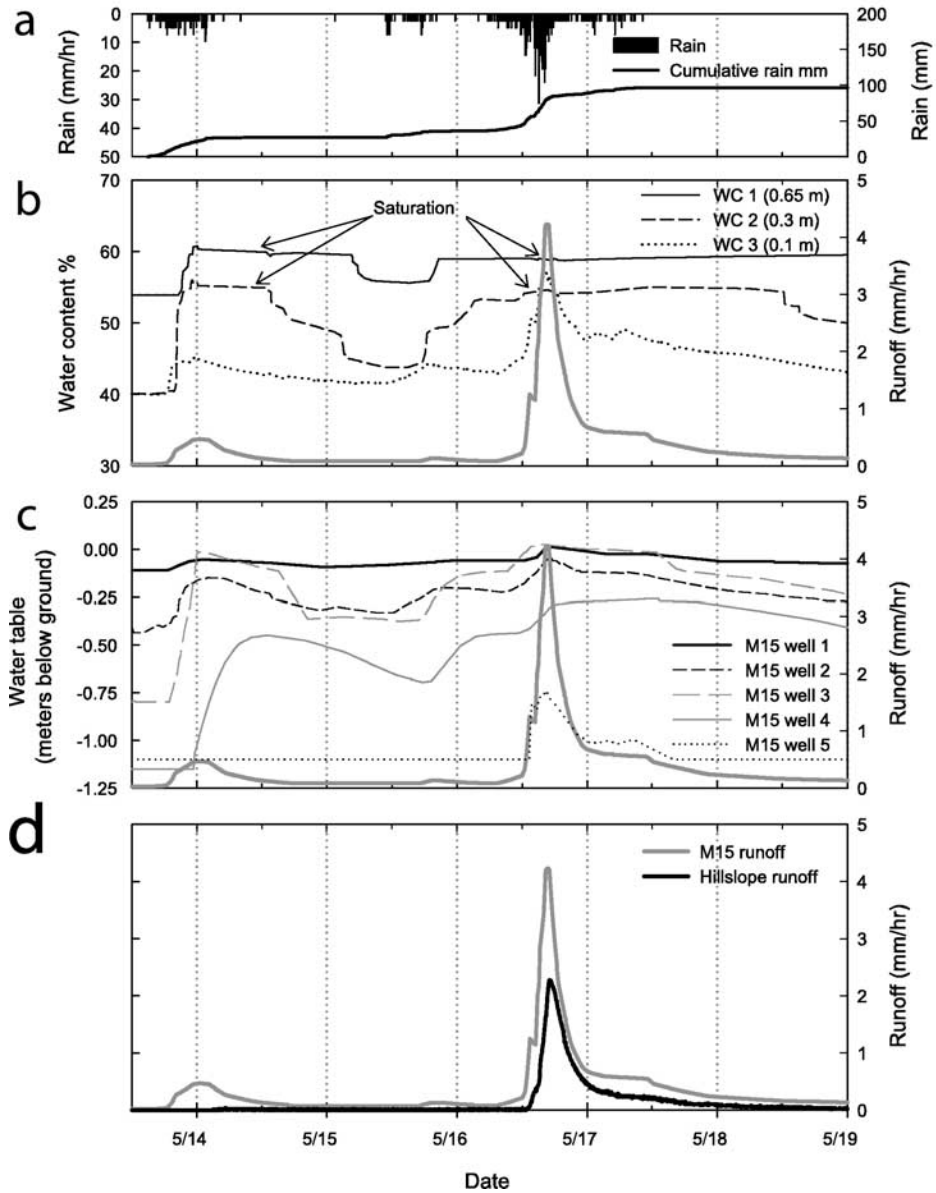

Figure 4. (a) Rainfall hyetograph and cumulative rain for events 1 and 2. (b) Riparian water content probe nest located near the break in slope between the hillslope and riparian zone in the M15 catchment. (c) Water table time series for wells located in the M15 catchment. Wells 1–3 are located in the riparian zone, and wells 4 and 5 are located in hillslope positions. Wells are ordered in the legend from nearest to farthest from the stream channel. (d) M15 catchment runoff and gauged hillslope runoff time series.

phase of the M15 hydrograph recession, hillslope water formed the majority of runoff, although once runoff receded to 0.6 mm on 17 May, hillslope and riparian runoff contributed equally to catchment runoff. From 18 May to the return to base flow conditions, the hillslope proportion of total flow decreased at a decreasing rate while riparian water contributions remained steady, reaching 100% of catchment runoff by the middle of 19 May.

[33] The relationship between M15 runoff sources (hillslope and riparian zones) was strongly hysteretic (Figure 5a and later results section). The bivariate plot of hillslope runoff versus riparian runoff showed counterclockwise hysteresis through time, with riparian runoff dominating the rising limb of the hydrograph and hillslope runoff dominating the falling limb. The hysteretic nature of M15 runoff sources demonstrates threshold behavior in catchment runoff sources and the nonsteady state behavior of discretized landscape unit hydrology: Hillslope and riparian zones did not respond to precipitation following steady state principles; rather, the relationship was variable and threshold mediated.

5.4. The $\delta^{18}O$ Dynamics in Precipitation, Streamflow, and Hillslope Runoff

[34] The $\delta^{18}O$ of M15 catchment runoff at base flow was consistently −6‰ for the 3 weeks prior to event 1, which matched $\delta^{18}O$ measured in riparian wells and lysimeters (Figure 6). Precipitation $\delta^{18}O$ measured sequentially in 5-mm intervals in event 1 decreased monotonically from

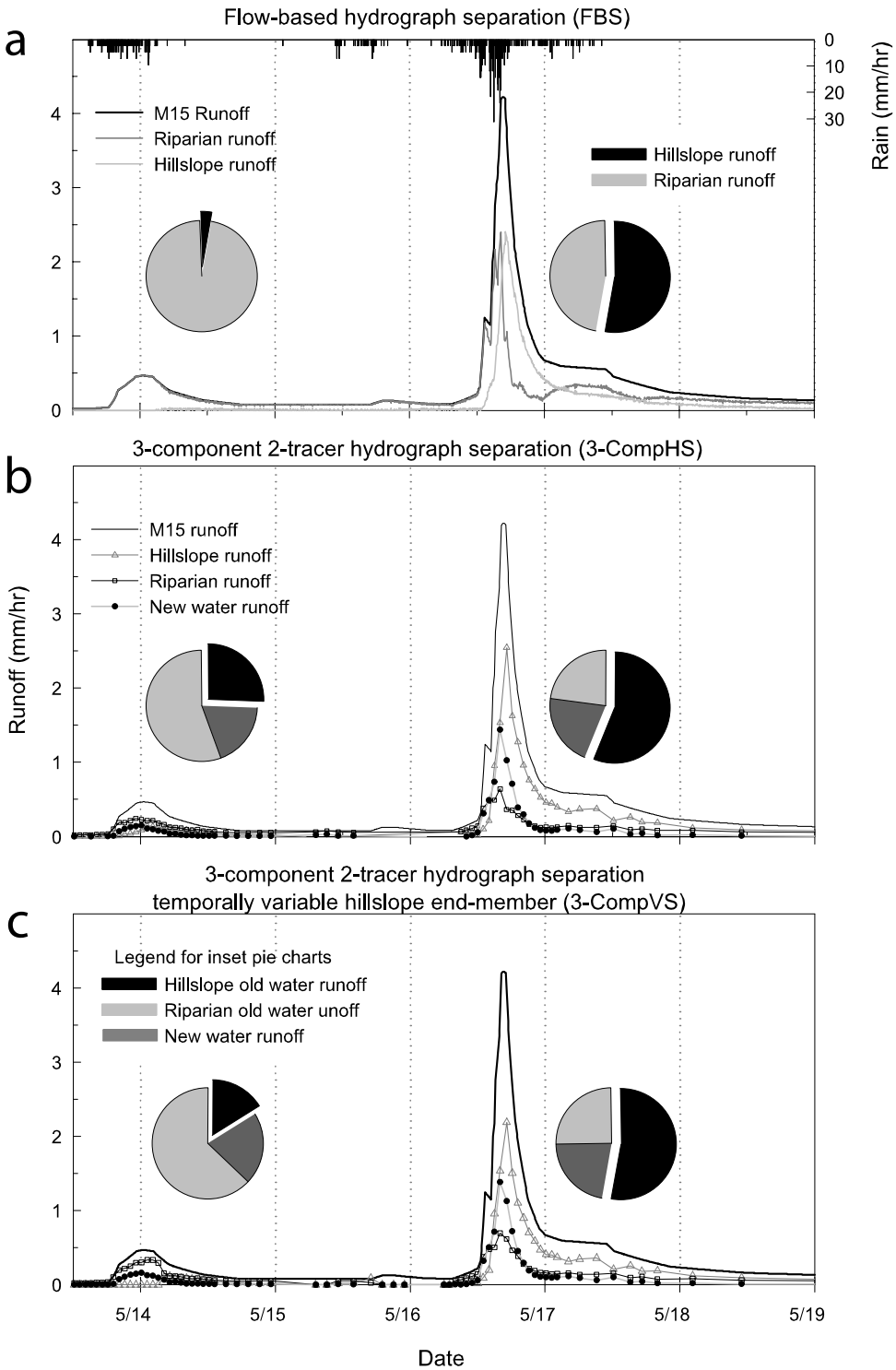

Figure 5. (a) Flow-based hydrograph separation of M15 catchment runoff into riparian and hillslope source water for events 1 and 2. Pie charts represent the relative proportions of hillslope (shaded) and riparian zone (solid) water in M15 catchment runoff for events 1 and 2. (b) Three-component hydrograph separation of M15 catchment runoff for events 1 and 2. Pie charts represent relative proportions of the three runoff components. (c) Three-component hydrograph separation of M15 catchment runoff for events 1 and 2 with a time varying hillslope component. Pie charts represent relative proportions of the three runoff components. Note the similar proportions of hillslope runoff and combined old riparian and new water runoff in all three separation approaches (Figures 5a–5c) in event 2.

Table 3. Hydrograph Separation Model Summaries[a]

	Method			
	Flow-Based Separation (Hillslope/Riparia) (FBS)	Two-Component Separation (New/Old Water) (2CompHS)	Three-Component Separation (New/Old Riparian/Old Hillslope) (3CompHS)	Three-Component Separation-Time Varying Hillslope Component (New/Old Riparian/Old Hillslope) (3CompVS)
Event 1	3%/97%	22%/78%	19%/55%/26%	21%/63%/16%
Event 2	47%/53%	30%/70%	21%/23%/56%	22%/25%/53%
Hillslope event 1	3%	4%/96%	26%	16%
Hillslope event 2	47%	7%/93%	58%	55%
Riparian event 1	97%	17%/83%	74%	84%
Riparian event 2	53%	47%/53%	42%	45%

[a]Percentage estimates for each component are approximations only and do not incorporate uncertainty estimations.

−2.3 to −3.3‰ (weighted values), providing for a strong unambiguous separation between new and old water components. Streamflow $\delta^{18}O$ responded quickly to enriched precipitation $\delta^{18}O$, indicating new water mixing in catchment runoff. The values then became more depleted, reflecting hillslope $\delta^{18}O$ values (−5.7‰), leveled off beginning on 14 May at 1200 LT, and then returned to pre-event concentrations by 15 May at 0600. The minimal amounts of observed hillslope runoff $\delta^{18}O$ remained steady at −5.7‰, indicating essentially no new water present in hillslope runoff.

[35] The $\delta^{18}O$ values in event 2 precipitation were initially close to stream values (−5.6 versus −6.0‰) in the low intensity first 5 mm of rain. Rainfall $\delta^{18}O$ became more enriched as more rain fell and intensity increased. Maximum separation of −2.75‰ (weighted value) between rain and pre-event base flow was achieved at peak runoff (Figure 6). M15 runoff $\delta^{18}O$ responded slightly to initial event 2 precipitation despite poor separation between the signals. Hydrograph uncertainty was high in the interstorm period as a result of the similarity between event 2 initial precipitation and old water $\delta^{18}O$ values; however, good separation between precipitation and runoff $\delta^{18}O$ was achieved with subsequent precipitation.

[36] Peak $\delta^{18}O$ values in event 2 runoff were similar to $\delta^{18}O$ response in event 1. Notwithstanding, recovery following precipitation cessation was more prolonged in event 2 and again plateaued at hillslope runoff $\delta^{18}O$ values before fully returning to riparian/groundwater signatures. Prolonged isotopic recession toward pre-event signatures suggests delayed new water contributions and new/old water mixing in the riparian zone. Hillslope runoff $\delta^{18}O$ was nearly constant with maximum deflection toward precipitation of 0.2‰ at peak runoff, signifying a consistent old water hillslope runoff signature.

5.5. Two-Component Hydrograph Separations (2-CompHS)

[37] Two-component hydrograph separations of hillslope runoff into new and old water components resulted in 96% old water in event 1 and 93% old water in event 2 (Figure 7, Table 3). We observed negligible hillslope runoff in event 1 and substantial runoff in event 2. Both separations show overwhelming dominance of old water and small proportions of new water in hillslope runoff during both low and high hillslope runoff conditions. Peak hillslope runoff in event 1 was composed of 96% old water, and peak hillslope runoff in event 2 was 90% old water with a minimum old water proportion (88%) 1 hour prior to peak runoff.

[38] We conducted two-component hydrograph separations of M15 catchment runoff into new and old water components discretely for events 1 and 2 (Figure 7). Old water formed the majority of runoff for both events 1 and 2 (78% and 70%, respectively) (Table 3). At peak runoff in event 1, old water formed 65% of total catchment runoff, synchronous with a new water peak of 35%. In event 2, old water again formed 65% of peak catchment runoff. However, in event 2, a maximum new water contribution of 47% preceded the runoff peak by 1 hour.

5.6. Combined Flow-Based and Two-Component Hydrograph Separations

[39] We combined our flow-based hydrograph separation model (FBS) with a tracer-based two-component hydrograph separation model (2-compHS) to determine old hillslope, new hillslope, old riparian, and new riparian runoff contributions to total catchment runoff. On the basis of the flow-based hydrograph separation that quantified the runoff from riparian zones and hillslope zones, and two-component hydrograph separations of gauged hillslope runoff and total M15 catchment runoff, we estimated the new and old water contributions from the riparian zone in the M15 catchment (Figure 8). We found that a negligible amount of catchment new water originated in hillslope zones during event 1 (1%) and a minor amount in event 2 (11%) (Figure 8a and Table 4). Hillslope zones contributed 3% and 62% of the total old water observed at the catchment outlet in events 1 and 2, respectively.

[40] Riparian runoff, however, contributed 97% of the old water and 99% of the new water in event 1 and 38% of the old water and 89% new water in event 2 (Figure 8a and Table 4). The old water proportion of riparian runoff was greatest early on the rising limb and on the end of the falling limb of each event hydrograph. In event 1, 99% of new water present at the M15 catchment outlet originated in riparian zones. In the larger second event, 89% of new water originated in the riparian zone. Although hillslope runoff comprised roughly half the runoff in event 2, it did not supply significant new water to catchment runoff. In event 2, hillslope runoff contributed 62% of total catchment old water runoff.

5.7. Silica Dynamics in Streamflow and Hillslope Runoff

[41] Hillslope runoff Si levels were constant at 91 μmol/L throughout event 1. They declined to 84 μmol/L between events and then rebounded to 90 μmol/L prior to the event 2 dilution response. Concentrations declined to 70 μmol/L at

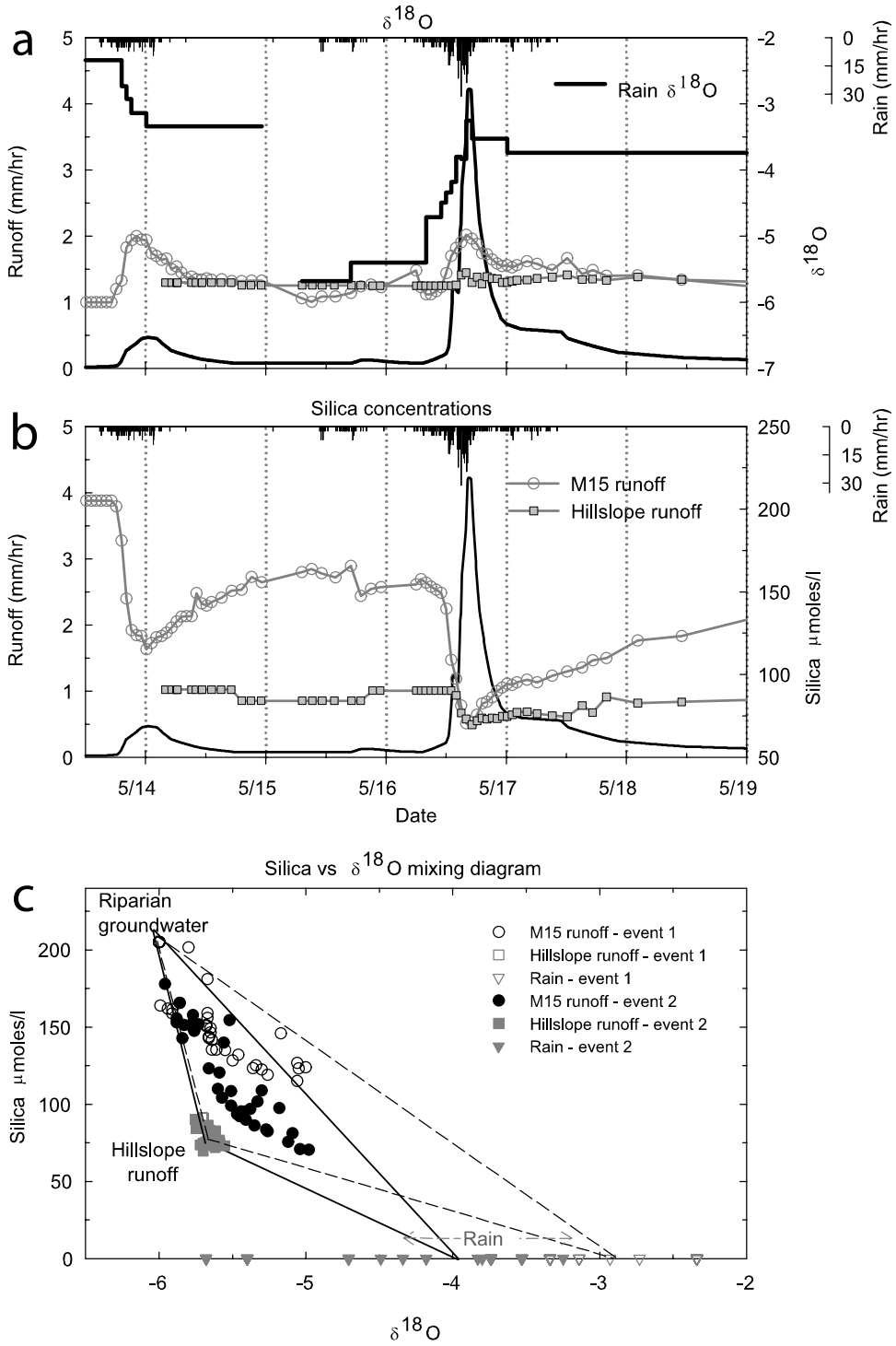

Figure 6. (a) Incrementally weighted rain $\delta^{18}O$ time series for events 1 and 2, M15 catchment runoff $\delta^{18}O$ time series, gauged hillslope runoff $\delta^{18}O$ time series, and M15 catchment runoff. (b) Silica concentration time series of M15 catchment runoff and gauged hillslope runoff. (c) Silica versus $\delta^{18}O$ mixing diagram. Catchment runoff source waters form the corners of the solid and dashed triangles that represent events 1 and 2, respectively. Catchment runoff for events 1 and 2 is shown by open and solid circles.

peak runoff coincident with M15 increases in streamflow (Figure 6b). Hillslope Si concentrations recovered to pre-event levels by 18 May.

[42] Silica concentrations in M15 catchment pre-event base flow were steady at 205 μmol/L and corresponded to riparian/groundwater sampled in wells and lysimeters (Figure 6b). In response to precipitation, M15 Si concentrations decreased to nearly 57% of pre-event levels at peak runoff, recovering more slowly than they decreased, to concentrations 80% of pre-event base flow concentrations.

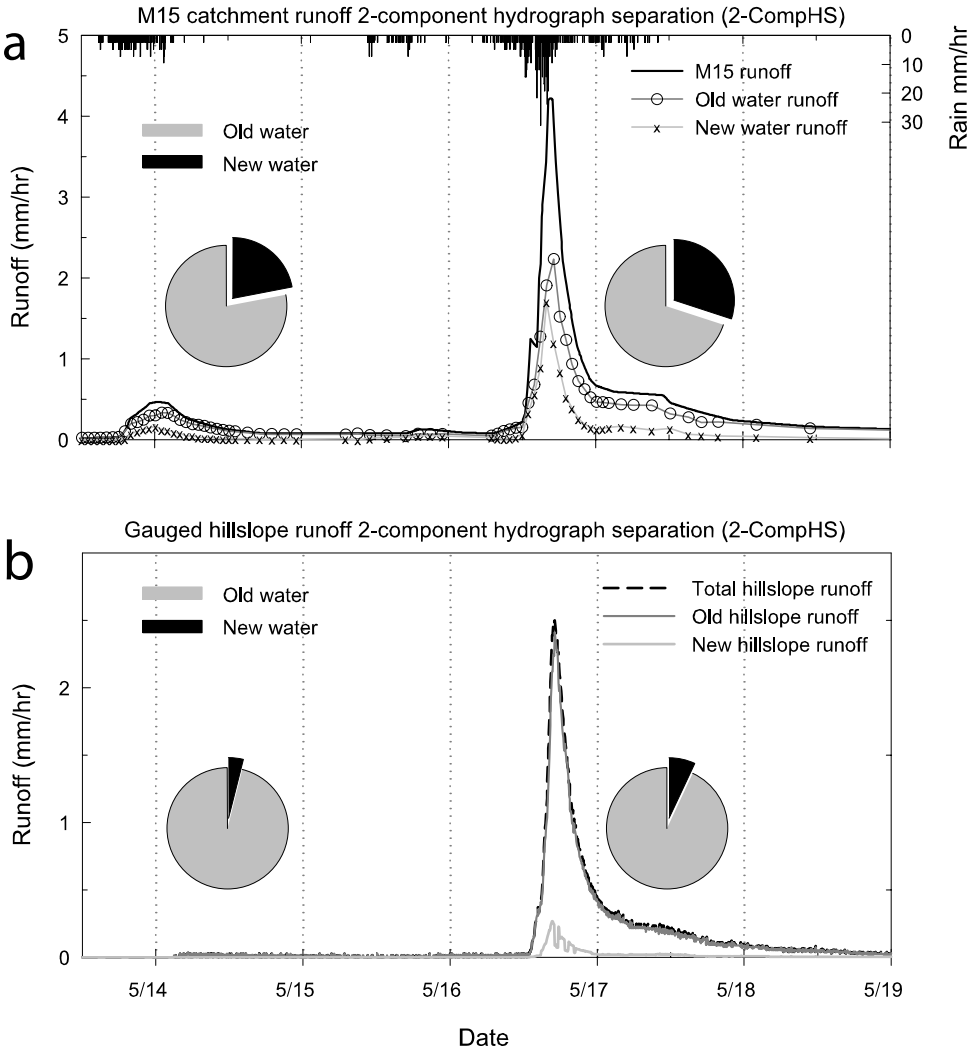

Figure 7. (a) Two-component temporal hydrograph separations of M15 catchment runoff into new and old water. Pie charts represent the relative proportions of new (solid) and old water (shaded) for events 1 and 2. (b) Two-component temporal hydrograph separations of gauged hillslope runoff into new and old water. Pie charts represent the relative proportions of new (solid) and old water (shaded) for events 1 and 2. Note the small proportion of new water in hillslope runoff in both events.

Base flow prior to event 2 was 165 μmol/L; it responded slightly to the first low-intensity initial precipitation and demonstrated a more pronounced dilution response to the main precipitation burst. M15 Si was most dilute at the catchment runoff peak. In event 2, M15 streamflow Si concentrations converged on and matched hillslope Si signatures at peak flow. This corresponded to high hillslope runoff proportions estimated with the FBS model at peak flow and additional silica dilution by new rainwater. Recovery to pre-event Si levels was slow and by 24 May was still only 178 μmol/L, 27 μmol/L less than pre-event 1 base flow. Bivariate plots of M15 runoff show hysteresis in the relationship between stream silica concentrations and M15 runoff (Figure 9). In both events, silica concentrations were higher on the rising limb than the falling limb at the same discharge, resulting in clockwise hysteresis.

5.8. Combined $\delta^{18}O$ and Si Observations

[43] The $\delta^{18}O$ provided for separation of old water and new water sources of runoff (temporal sources). Since silica concentrations were significantly greater in riparian zones than hillslope zones, silica provided for separation of riparian and hillslope runoff contributions to catchment runoff (spatial sources). Combined, these naturally occurring tracers allowed separation of new and old water and the further separation of old water into old hillslope and old riparian source water components. The bivariate mixing diagram of Si versus ^{18}O shown in Figure 6c shows the relationship between $\delta^{18}O$ and Si for each of the major catchment landscape units and precipitation. The M15 runoff samples fall mainly within the mixing triangles superimposed on Figure 6c. At base flow prior to event 1, streamflow was comparable to riparian water. Catchment runoff samples traversed the mixing space between the end-members (components) through the event, demonstrating the changing contributions of new, old hillslope, and old riparian water through time. The shape of the mixing triangles changed through the event as the rain end-member composition (bottom right corner of the triangle) shifted through time. These mixing triangles formed the basis of the

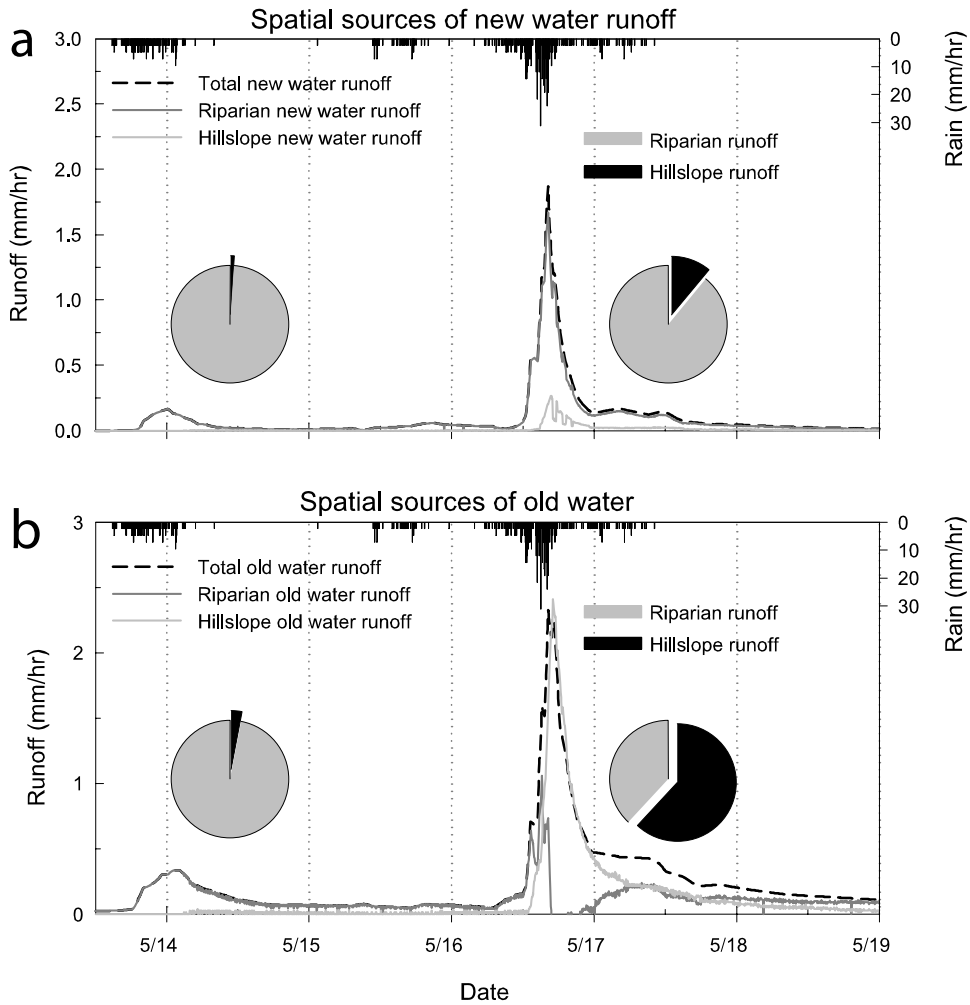

Figure 8. (a) Spatial sources of the new water runoff component of M15 catchment runoff. Pie charts represent relative proportions of hillslope (solid) and riparian (shaded) sources of new water. (b) Spatial sources of old water runoff component of M15 catchment runoff. Pie charts represent the relative proportions of hillslope (solid) and riparian (shaded) sources of old water.

three-component hydrograph separations outlined in the following sections.

5.9. Three-Component Hydrograph Separations

[44] Three-component tracer-based hydrograph separations were performed separately for each monitored event. We found that each component contributed to streamflow in event 1. Riparian water contributions to total storm runoff were 55% of total flow. Hillslope contributions were 26%, and new water comprised 19% of total runoff (Figure 5b, Table 3). At peak runoff, riparian, hillslope, and new water contributions were 46%, 34%, and 20%, respectively. Both riparian and new water contributions peaked prior to the streamflow peak (2 hours and 1 hour, respectively), with hillslope contributions peaking coincidentally with M15 runoff. Riparian contributions dominated M15 runoff and were greatest on the rising limb of the event hydrograph.

[45] The three-component hydrograph separation for the initial rainfall associated with the second event was poor due to poor separation among the end-members. The $\delta^{18}O$ values in initial event 2 rain were similar to stream and hillslope runoff signatures, invalidating the separation. However, after the second 5 mm of rain, the difference between the end-members was greater and a valid separation became possible (Figure 6). The riparian source component responded most quickly to the main burst of event 2 rain, followed quickly by the new water component. The hillslope contribution to catchment runoff was lagged more than 5 hours, but once initiated, increased rapidly and dominated catchment runoff. Only 3 hours passed from hillslope runoff initiation until hillslope runoff formed the majority of total catchment runoff. Riparian runoff peaked at 16 May, 1600 LT, 1 hour before streamflow peaked, and decreased as hillslope runoff proportions continued to

Table 4. Spatial Sources of New and Old Water in the M15 Catchment Based on the Hydrological Hydrograph Separation and Tracer Based Two-Component Hydrograph Separation Models[a]

Temporal Sources	Event 1 (Hillslope/Riparian)	Event 2 (Hillslope/Riparian)
New	1%/99%	11%/89%
Old	3%/97%	62%/38%

[a]Percentage estimates for each component are approximations only and do not incorporate uncertainty estimations.

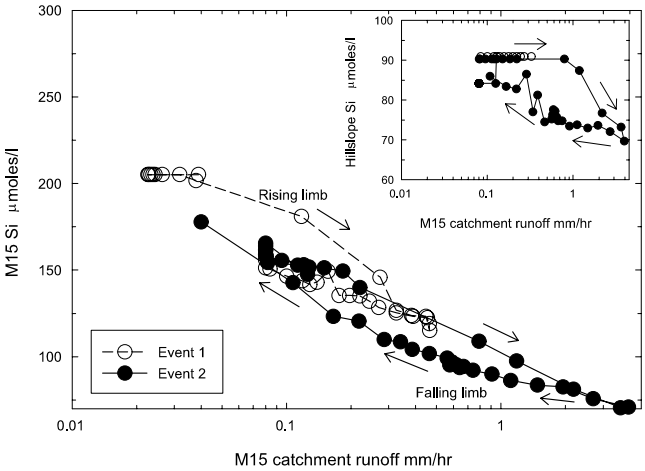

Figure 9. Silica concentrations versus M15 catchment runoff. Note clockwise hysteresis in both events 1 and 2 (shown with open and solid circles). The inset graph is hillslope runoff silica concentration versus M15 catchment runoff.

increase. Hillslope runoff peaked within 0.5 hours of catchment runoff and subsequently decreased at a rate comparable to catchment runoff recession. New water peaked coincidentally with riparian runoff, 1 hour prior to catchment runoff and decreased rapidly until 16 May, 2100 LT, when new water runoff and riparian runoff proportions were comparable and hillslope runoff comprised 69% of total streamflow. Hillslope runoff continued to decline until 19 May, when hillslope and riparian contributions to streamflow became equal.

5.10. Temporally Variable Hillslope End-Member Three-Component Hydrograph Separation

[46] Three-component tracer based hydrograph separations were performed with the hillslope runoff component as a temporally variable end-member based on observed hillslope runoff signatures (Figure 5c). In this model, separation was constrained to two end-members (new water and riparian water) until runoff from the hillslope was measured; thereafter all three-components (including hillslope runoff) were included in the separation with recent hillslope runoff signatures applied. Hillslope runoff was not initiated until 14 May at 0400 LT. Consequently, in event 1, 63% of total runoff was attributed to the riparian zone, 21% to new water, and 16% to hillslope zones (Table 3). In event 2, the time varying hillslope end-member had less effect, with total runoff proportion from each component remaining within 3% of the standard three-component separation. Hillslope runoff was 3% less, riparian runoff 2% more, and new water 1% more than in the 3-compHS model. The most marked difference between the standard approach (3-CompHS) and the temporally variable hillslope end-member approach (3-CompVS) was at peak runoff, where the hillslope component was reduced from 60% to 52% of total M15 runoff (Table 3).

5.11. Model Comparison

[47] Table 3 provides a summary of each model applied and the spatial and temporal source estimates provided by each method. Uncertainty estimates were calculated for the flow-based hydrograph separation method and the temporally variable hillslope end-member three-component hydrograph separation (3-CompVS) [*Genereux*, 1998]. Comparison of estimated hillslope runoff (Figure 10), including associated uncertainty, shows consistency between the models (r^2 = 0.91). The regression was computed for both events 1 and 2 combined. The hydrological hydrograph separation is a hydraulic model. Conversely, the tracer based 3-CompVS model is particle-based. The greatest divergence in the estimates made by the two models occurred with the displacement/mixing of riparian water with hillslope runoff into the riparian zone. While the hydrological separation assumes instantaneous displacement, the tracer-based model indicates that mixing occurs (Figure 11). The falling limb of the riparian runoff contribution to total runoff demonstrates this difference. In the FBS model, the falling limb is abrupt, while the falling limb is more extended in the tracer-based model.

5.12. Relative Timing of Hillslope, Riparian, and New Water Contributions to Runoff

[48] In each runoff source water model applied to event 2 (FBS, 2-CompHS, 3-CompHS, 3-CompVS), riparian runoff response was the first to contribute to catchment runoff, followed by new water, and finally hillslope runoff. Riparian and new water were well correlated and proportionally greatest on the rising limb with hillslope runoff lagged and greatest near peak runoff and on the initial phase of the hydrograph recession, as shown by time series hydrograph separations in Figure 5.

[49] On the basis of flow-based separation (FBS), the relative timing of hillslope and riparian runoff is clearly demonstrated by the hysteretic nature of bivariate plots of source contributions to catchment runoff (Figure 12). On the

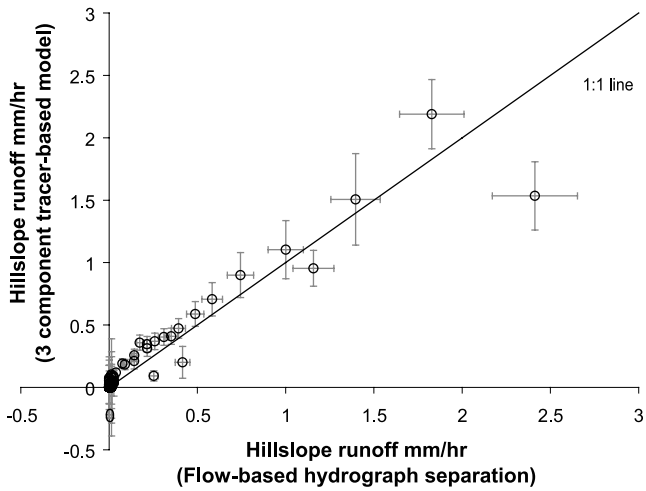

Figure 10. Bivariate plot of hillslope runoff estimated with the tracer-based three-component two-tracer mixing model (3-CompHS) and hillslope runoff estimated with the flow-based hydrograph separation model (FBS). Horizontal uncertainty bars are a constant 10% of estimated runoff for the flow-based approach. Vertical uncertainty bars are a function of analytical precision of end-member tracer samples and uncertainty propagation through the three-component two-tracer mixing model (3-CompHS) following the procedure outlined by *Genereux* [1998].

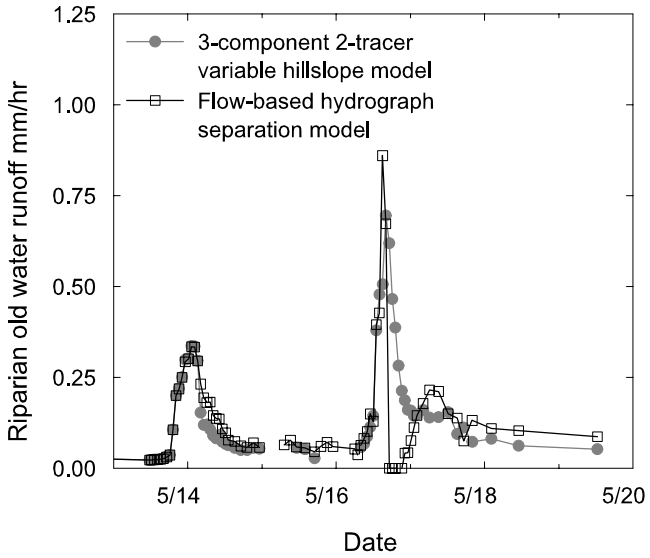

Figure 11. Time series comparison of riparian runoff estimates based on the FBS model and the 3-CompHS model. Note the difference in the recession estimates for the second hydrograph peak. The FBS model assumes instantaneous displacement of riparian water by hillslope water, while the tracer-based model suggests a degree of mixing.

rising limb of the event hydrograph, hillslope runoff is proportionately smaller as compared to the same M15 catchment runoff on the falling limb, resulting in counterclockwise hysteresis. Conversely, riparian runoff is proportionately greater on the rising limb of the event hydrograph than at the same M15 catchment runoff on the falling limb, resulting in clockwise hysteresis. The relative timing of riparian and hillslope runoff contributions to total M15 catchment runoff are most clearly demonstrated in Figure 12c, where riparian runoff is much greater on the rising limb and hillslope runoff is much greater on the falling limb. This is shown by pronounced clockwise hysteresis in the riparian to hillslope runoff bivariate plot. Each plot included in Figure 12 demonstrates that riparian runoff dominates the rising limb of the M15 event hydrograph and hillslope runoff dominates the falling limb.

[50] The lag in hillslope runoff contributions to catchment runoff coupled with rapid riparian runoff response result in clockwise hysteresis in the bivariate plot of silica concentration versus M15 catchment runoff (Figure 9). Since riparian zone silica concentrations were roughly double hillslope zone concentrations, clockwise hysteresis in riparian to hillslope runoff results in clockwise hysteresis in the silica to

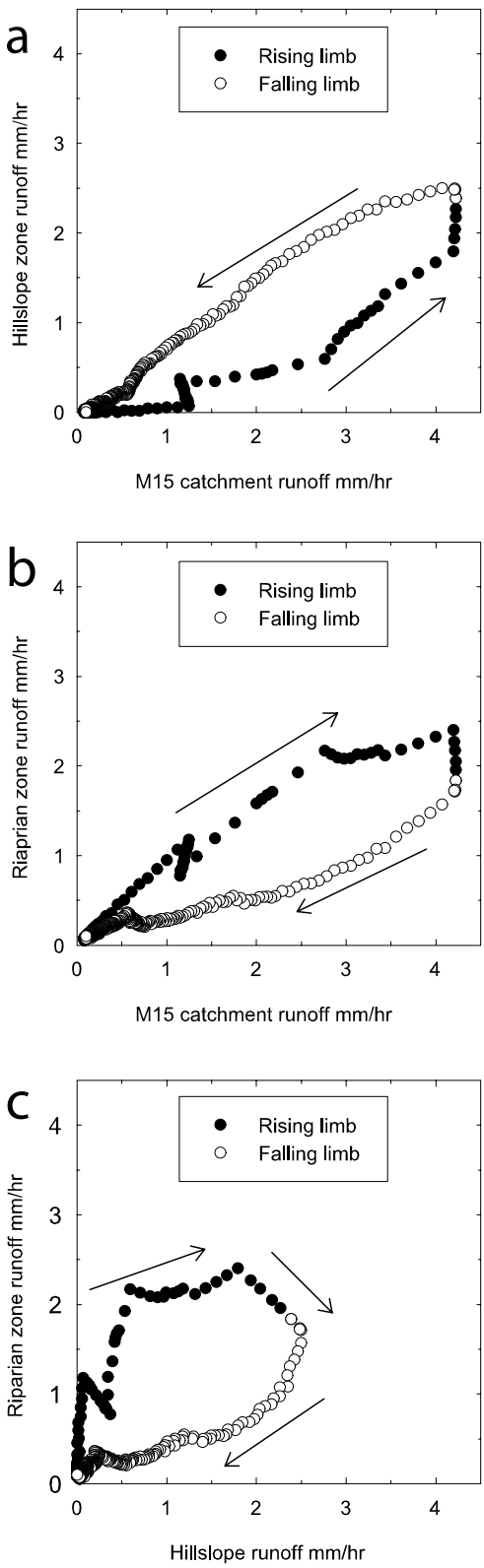

Figure 12. (opposite) (a) Gauged hillslope runoff versus M15 catchment runoff for events 1 and 2. Rising limbs of the hydrographs are shown as solid circles, and falling limbs are shown as open circles. Note counterclockwise hysteresis in the relationship with relatively little hillslope runoff for a given M15 catchment runoff on the rising limb as compared to the same M15 catchment runoff on the falling limb. (b) Calculated riparian runoff versus M15 catchment runoff for events 1 and 2. Note the clockwise hysteresis in the relationship demonstrating greater riparian runoff for a given discharge on the rising limb as compared to the same discharge on the falling limb. (c) Riparian runoff versus hillslope runoff for events 1 and 2. Minimal hillslope runoff was present in event 1. Note clockwise hysteresis in the relationship with relatively little hillslope runoff for a given riparian runoff on the rising limb as compared to the same riparian runoff on the falling limb.

M15 catchment runoff relationship. New water contributions were greatest on the rising limb of the M15 catchment runoff hydrograph (coincident with riparian old water contributions) and resulted in "flattening" of the hysteretic relationship through dilution of the riparian runoff silica signal. Despite the new water dilution effect on the rising limb, the relative proportions of riparian and hillslope runoff through the event were nonetheless sufficient to result in a hysteretic relationship between catchment runoff silica concentrations and catchment runoff rates.

6. Discussion

6.1. Does Mapped Riparian Extent Equal the Computed New Water Contribution?

[51] The 2.6-ha M15 catchment is composed of 97% hillslope zones, 2% riparian zones, and 1% stream channel zones as mapped based on soils, topography, proximity to the channel, and geomorphic form (Table 1). This static mapping exercise was a conservative first-order approximation of riparian zone extent for discretization of the M15 watershed into dominant landscape units (hillslopes and riparian zones). We found a runoff ratio (R = runoff/precipitation) of 0.55 for the M15 catchment in event 2. M15 catchment runoff was 71% old water and 29% new water. Our isotopic hydrograph separations at the hillslope scale indicated that 93% of total hillslope runoff was old water. Conservatively mapped valley bottom riparian zones could account for a maximum of 13% of M15 new water runoff, assuming direct precipitation onto saturated near-stream zones and transport to the stream channel. New hillslope water runoff can account for 11% of M15 new water runoff. Estimated direct channel interception of rainfall accounts for 6% of total new water runoff. In total, directly measured new water accounts for 30% of the total new water observed at the catchment outlet.

[52] We found that 70% of the new water observed at the catchment outlet was derived from zones intermediate between the valley bottom riparian zone and the monitored hillslope zone. Assuming that this remaining 70% new water was direct precipitation onto saturated or near-saturated areas, an additional 3,280 m^2 or 12.5% of the catchment area comprised a dynamic variably saturated lower hillslope and zero-order hollow zone. We have known this variable saturated area process for many years [*Hewlett and Hibbert*, 1967; *Dunne et al.*, 1975]; however, these data quantify this dynamic zone directly. An expanding saturated zone up onto the lower hillslopes, up into the larger hollows, and into ephemeral channels comprised an area between the monitored hillslope terminus and the measured valley bottom extent. Our quantitative results demonstrate the surface saturated extent of *Sidle et al.*'s [2000] qualitative observation of progressive contributions from hydrogeomorphic units beginning low in the catchment and finishing with lower slopes and zero-order hollows during highest catchment runoff. Our results also quantify the surface saturated extent of the subsurface contributing area findings of *Anderson et al.* [1997]. The expanding saturated zone was consistent with water table dynamics observed in lower hillslope and lower hollow zones in the Maimai catchments. Water tables on hillslopes were transient, with water tables at or near the ground surface commonly measured on lower hillslopes and up into zero-order hollows throughout the Maimai catchments in response to precipitation.

[53] We have struggled with the relative roles of valley bottom zones and hillslope runoff in new water runoff production for many years. Variable saturated area theory has been invoked to explain observed percent new water in catchment runoff with the assumption that hillslope runoff was all old water. Often, these assumptions were made without corroboration of observed hillslope runoff composition, mapped valley bottom area, mapped channel area, and observed lower hillslope saturation. *Pearce et al.* [1986] and *Sklash et al.* [1986] found new water contributions of 15–25% of total catchment runoff during three monitored 33 to 44 mm rain events at Maimai. Similarly, Sklash and Pearce stated that the monitored new water could be explained by flow from 10% of the catchment area (saturated area), an area estimate larger than the 4–7% of the catchment estimated as capable of generating overland flow [*Pearce and McKerchar*, 1979; *Mosley*, 1979]. In the current study, we have quantified channel area and valley bottom zones and find that riparian area estimates based on new water percentages exceed mapped channel and valley bottom area. Because we simultaneously monitored hillslope runoff composition, including new water percentages, we were able to quantify variable source area expansion and new water contributions from zones intermediate between hillslopes and valley bottoms. Our observations quantify, for the first time, the new water contributions from hillslopes, riparian zones, and the dynamic variable source areas that extend onto lower portions of hillslopes and into zero-order hollows, forming a shifting interface between the hillslopes and riparian areas in headwater catchments.

6.2. Catchment Runoff: Hillslope Water or Displaced Riparian Zone Water?

[54] We found that 99% of new water arriving at the catchment outlet during event 1 originated in the riparian zone (Figure 8, Table 4). Despite the majority of catchment runoff originating in hillslope positions in event 2 (based on combined FBS and 2-CompHS approaches), riparian and VSAs contributed 89% of catchment new water. Near-stream, lower hillslope, and lower hollow water tables rose to the soil surface and suggested saturation excess overland flow and rapid shallow throughflow of new water. Isotopic sampling of near-stream wells and lysimeters further suggested shallow or overland flow pathways of new water due to little deflection of riparian groundwater toward rain $\delta^{18}O$ signatures. These results are consistent with riparian flow path stratification found by *McGlynn et al.* [1999] in riparian areas during snowmelt at Sleepers River, Vermont. Despite the steep, highly responsive subsurface runoff nature of the Maimai catchments, the dynamic riparian area appears to control new water contributions to catchment runoff.

[55] The spatial sources of old water were a function of event size and antecedent moisture conditions. Since a hillslope runoff threshold was not attained in event 1, 74–97% of old water catchment runoff was generated in riparian zones, depending on the separation method applied (Table 3). However, in event 2, where hillslope runoff was a factor, only 22–38% of old water catchment runoff originated in riparian zones; the remaining 62–78% originated in hillslope positions (Table 3).

[56] The relative timing of new water contributions and spatial sources of old water runoff are perhaps more informative of catchment controls on runoff generation than absolute runoff proportions. The new water component in catchment runoff was greatest early in the hydrograph, peaking before catchment runoff in both events, and was similar in timing to riparian old water contributions. This appears to be a result of the riparian and lower hillslope generation of most of the new water runoff and the associated short and rapid flow paths to the stream channel. Rapid shallow flow paths and riparian source areas for new water runoff generation are significant for export of dissolved organic carbon and other solutes associated with shallow riparian soils [*McGlynn et al.*, 1999]. We would expect that these solutes would exhibit hysteretic relationships to catchment runoff, with higher concentrations on the rising limb of the event hydrograph than on the falling limb due to the early timing of riparian new and old water runoff as compared to total catchment discharge. In fact, *Moore* [1989] and *McGlynn and McDonnell* [2003] found that dissolved organic carbon (DOC) concentrations were higher on the hydrograph rising limb than on the falling limb in multiple Maimai headwater catchments. These results also suggest that most of the 22–30% of new water that makes it to the catchment outlet during events has little contact with subsurface soils and little time for chemical weathering reactions.

[57] Riparian old water, regardless of the mixing model, was well correlated to new water runoff, was greatest on the rising limb, and peaked prior to catchment runoff. Hillslope contributions lagged riparian new and old water (Figure 5) as demonstrated in Figure 12c, showing riparian versus hillslope runoff. The relative timing of riparian and hillslope runoff suggests that hillslope runoff displaces riparian water once hillslope runoff is initiated. Riparian water arrives at the catchment outlet prior to hillslope runoff because of its near-channel discharge position, rapid water table response to precipitation, and displacement by mobile hillslope runoff following threshold-mediated hillslope water table development.

[58] Riparian zones and hillslope zones did not contribute equally to catchment runoff. Runoff ratios (R = runoff/rainfall) for hillslope zones, riparian zones, and the M15 catchment show the proportion of precipitation falling on a landscape unit relative to total runoff from that unit. Hillslope zones during the first 27-mm event contributed minimal proportions of incident precipitation to runoff (R = 0.01). M15 runoff ratios (R = 0.25) far in excess of hillslope runoff ratios indicated that riparian zones contributed more substantially. Hillslope runoff ratios increased from 0.01 to 0.25 from event 1 to 2, demonstrating the wetting up of hillslope positions. Catchment runoff ratios also increased from 0.25 to 0.55, incorporating increased runoff ratios from both riparian zones and hillslope zones.

[59] These observations quantify the dynamics hypothesized by *Hewlett and Hibbert* [1967] and suggested by *Sidle et al.* [2000]. However, we found that the sequencing of landscape unit contributions to catchment runoff was threshold mediated. Hewlett and Hibbert suggested that runoff ratios would decrease in an upslope direction away from the stream channel. They hypothesized that upslope positions contributed to lower catchment runoff ratios, with upslope zones sustaining base flow between events. *Sidle et al.* [2000] also described a progressive wetting up from valley bottom zones to zero-order hollows with successive storm events as catchment wetness increased through a monsoon season in Japan. At Maimai, we found threshold mediated runoff responses from dominant landscape positions. The small event and early portions of the large event were dominated by riparian runoff. As runoff increased in the second event, hillslope runoff was initiated and riparian water was displaced into the stream. Hillslope runoff became the dominant contributor to total runoff near the hydrograph peak and until late in the recession when proportions of riparian and hillslope runoff became equal. Our results allowed us to quantify the sequencing of contributions from catchment source areas through two storm events, through the progressive increase in catchment moisture status, and subsequent increases in catchment runoff.

6.3. What Controls C-Q Hysteresis?

[60] Hysteresis in solute-runoff (C-Q) relationships has received significant attention in recent research [*Creed et al.*, 1996; *Boyer et al.*, 1997; *Hornberger et al.*, 2001; *Scanlon et al.*, 2001]. *Scanlon et al.* [2001] and *Hornberger et al.* [2001] examined hysteresis in silica-discharge relationships in a headwater catchment in Virginia where modeled one-dimensional (1-D) water table fluctuations were hypothesized to control clockwise C-Q curves. Catchment runoff was monitored directly; however, the relative contributions of deep, shallow, and overland flow paths hypothesized to control silica concentrations and total runoff were based on model output, rather than on observed flow paths and volumes.

[61] At Maimai, we examined catchment runoff solute concentration hysteresis in addition to the hysteresis in spatial source runoff versus catchment runoff. We found, based on intensive hydrological monitoring and internal catchment source water sampling, that spatial (landscape unit) mixing controlled catchment runoff dynamics and observed hysteresis in stream discharge-silica relationships, rather than one-dimensional water table fluctuations. Clockwise hysteresis in the riparian runoff to hillslope runoff relationship and the counterclockwise hysteresis in the hillslope runoff to catchment runoff relationship demonstrated that riparian zone water dominated on the rising limb of the event 2 hydrograph and hillslope water dominated on the falling limb (Figure 12). Since Si concentrations were greater in the riparian zone than the hillslope zone, clockwise hysteresis in silica versus runoff was observed (Figure 9). This can be attributed to the timing of source water contributions. It is useful to note that where spatial sources of catchment runoff can be delineated and quantified, and where these spatial sources rather than 1-D water table dynamics are the controlling mechanisms, hysteresis may be explained by volumetric mixing of spatial source runoff components.

6.4. Does the Riparian Zone Buffer Hillslope Runoff?

[62] In the context of riparian zone hydrology, the term "buffer" can represent two distinct processes. First, volumetric buffering can refer to modulation of hillslope runoff through simple displacement or mixing that is partially

controlled by riparian reservoir size relative to inflow. Second, riparian buffering can refer to biogeochemical transformation of throughflow. In the context of this paper, we refer to volumetric buffering and the modulation of throughflow. We found that riparian zones were the sources of most new water runoff, and we inferred that new water flow paths were shallow and rapid based on new water response at the catchment outlet and a lack of lysimeter and well water deflection toward rainfall $\delta^{18}O$ values. At the Maimai M15 headwater catchment, we found that the riparian zone controlled runoff during a small event, between events, and in early portions of a large event. The amount, proportion, and timing of hillslope runoff that reached the catchment outlet were significantly different between the two monitored events. An earlier, greater amount, and larger proportion of total catchment runoff originated in hillslope positions in the larger, higher antecedent wetness event. During periods of hillslope runoff, the buffering potential of the riparian zone was a function of the riparian reservoir volume and hillslope throughflow to the riparian zone [*McGlynn and Seibert*, 2003]. We found indications that when the hillslope input exceeded the riparian zone storage volume, hillslope water displaced riparian water which reached the stream at rates comparable to hillslope runoff rates. However, because M15 catchment runoff returned to near pre-event silica signatures and did not remain at hillslope runoff silica levels, we inferred that not all riparian runoff was displaced. Rather, hillslope runoff bypassed some riparian zone positions either spatially through focused locations along the stream channel or via preferential flow pathways within the soil matrix. The 3-CompVS separations also suggested that mixing during displacement, as opposed to pure piston displacement as assumed by the FBS, occurred (Figure 11).

[63] The buffering of hillslopes by riparian zones in the M15 catchment depended on hillslope runoff relative to the volume of water stored in the riparian zone prior to the event. Greatest buffering occurred between events, during small events, and during early portions of large events. The riparian zones controlled new water runoff and exhibited poor buffering of hillslope throughflow once hillslope runoff was initiated in the large event (event 2). Buffering potential appears to be related to hillslope runoff rate/volume (throughflow) relative to the riparian reservoir size and flow paths through the riparian zone.

7. Conclusion

[64] We quantified the proportions of new water runoff from hillslopes, valley bottom riparian zones, channel areas, and intermediate zones of spatially and temporally variable saturation. We found that riparian water dominated between the events, throughout the small runoff event, and in early portions of the large event. In the large event, proportions of riparian and hillslope runoff were similar; however, riparian water was greater on the rising limb and hillslope water was greater on the falling limb. We also offer a comparison/test of a physical flow-based hydrograph separation and a tracer-based three-component hydrograph separation and demonstrate comparable results. During periods of hillslope runoff, the buffering potential of the riparian zone was a function of the riparian reservoir volume and hillslope throughflow to the riparian zone. Our approach allowed us to measure the spatial sources of new and old water through the monitored events and evaluate the roles of dominant landscape units in streamflow generation. While highly intuitive, these results are among the first to measure and model these component contributions directly. We believe that this is the first study to show unequivocally these separate contributions through an event, constrained by hydrometric, isotopic, and solute approaches.

[65] **Acknowledgments.** We extend our thanks to John Payne, Jagath Ekanayake, and Breck Bowden of LandCare Research, New Zealand, for logistical, technical, and collaborative support. We also thank Carol Kendall for isotope analysis and Rick Hooper, Jamie Shanley, Beth Boyer, and Jim Hassett for useful comments and discussion. This work was made possible by NSF grant EAR-0196381 and the 2001 American Geophysical Union Horton Research Grant awarded to B.L.M.

References

Anderson, S. P., W. E. Dietrich, R. Torres, D. R. Montgomery, and K. Loague, Concentration-discharge relationships in runoff from a steep, unchanneled catchment, *Water Resour. Res.*, *33*, 211–225, 1997.

Bazemore, D. E., K. N. Eshleman, and K. J. Hollenbeck, The role of soil water in stormflow generation in a forested headwater catchment: Synthesis of natural tracer and hydrometric evidence, *J. Hydrol.*, *162*, 47–75, 1994.

Becker, A., and P. Braun, Disaggregation, aggregation and spatial scaling in hydrological modeling, *J. Hydrol.*, *217*, 239–252, 1999.

Beven, K., and J. Freer, A dynamic TOPMODEL, *Hydrol. Processes*, *15*, 1993–2011, 2001.

Beven, K. J., and M. J. Kirkby, A physically based, variable contributing area model of basin hydrology, *Hydrol. Sci. Bull.*, *24*, 45–68, 1979.

Bonell, M., Selected challenges in runoff generation research in forests from the hillslope to headwater drainage basin scale, *J. Am. Water Resour. Assoc.*, *34*, 765–785, 1998.

Boyer, E. W., G. M. Hornberger, K. E. Bencala, and D. M. McKnight, Response characteristics of DOC flushing in an alpine catchment, *Hydrol. Processes*, *11*, 1635–1647, 1997.

Brammer, D., Hillslope hydrology in a small forested catchment, Maimai, New Zealand, M.S. thesis, Coll. of Environ. Sci. and For., State Univ. of New York, Syracuse, 1996.

Burns, D. A., J. J. McDonnell, R. P. Hooper, N. E. Peters, J. E. Freer, C. Kendall, and K. Beven, Quantifying contributions to storm runoff through end-member mixing analysis and hydrologic measurements at the Panola Mountain Research Watershed (Georgia, USA), *Hydrol. Processes*, *15*, 1903–1924, 2001.

Buttle, J., and J. J. McDonnell, Isotope tracers in catchment hydrology in the humid tropics, in *Forest-Water-People in the Humid Tropics*, edited by M. Bonell and L. A. Bruijnzeel, Cambridge University Press, New York, in press, 2003.

Christophersen, N., and R. P. Hooper, Multivariate analysis of stream water chemical data: The use of principal components analysis for the end-member mixing problem, *Water Resour. Res.*, *28*, 99–107, 1992.

Christopherson, N., C. Neal, R. P. Hooper, R. D. Vogt, and S. Anderson, Modelling streamwater chemistry as a mixture of soil water end-members—A step toward second-generation acidification models, *J. Hydrol.*, *116*, 307–320, 1990.

Creed, I. F., L. E. Band, N. W. Foster, I. K. Morrison, J. A. Nicolson, R. S. Semkin, and D. S. Jeffries, Regulation of nitrate-N release from temperate forests: A test of the N flushing hypothesis, *Water Resour. Res.*, *32*, 3337–3354, 1996.

DeWalle, D. R., B. R. Swistock, and W. E. Sharpe, Three-component tracer model for stormflow on a small Appalachian forested catchment, *J. Hydrol.*, *104*, 301–310, 1988.

Dunne, T., Field studies of hillslope flow processes, in *Hillslope Hydrology*, edited by M. J. Kirkby, pp. 227–293, John Wiley, Hoboken, N. J., 1978.

Dunne, T., and R. D. Black, An experimental investigation of runoff production in permeable soils, *Water Resour. Res.*, *6*, 478–490, 1970a.

Dunne, T., and R. D. Black, Partial area contributions to storm runoff in a small New England watershed, *Water Resour. Res.*, *6*, 1296–1311, 1970b.

Dunne, T., T. R. Moore, and C. H. Taylor, Recognition and prediction of runoff-producing zones in humid regions, *Hydrol. Sci. Bull.*, *20*, 305–327, 1975.

Genereux, D., Quantifying uncertainty in tracer-based hydrograph separations, *Water Resour. Res.*, *34*, 915–919, 1998.

Grayson, R. B., G. Bloeschl, and I. D. Moore, Distributed parameter hydrologic modelling using vector elevation data: Thales and TAPES-C, in *Computer Models of Watershed Hydrology*, edited by V. P. Singh, pp. 669–695, Water Resour. Publ., Highlands Ranch, Colo., 1995.

Hewlett, J. D., and A. R. Hibbert, Moisture and conditions within a sloping soil mass during drainage, *J. Geophys. Res.*, *68*, 1081–1087, 1963.

Hewlett, J. D., and A. R. Hibbert, Factors affecting the response of small watersheds to precipitation in humid areas, in *Forest Hydrology*, edited by W. E. Sopper and H. W. Lull, pp. 275–290, Pergamon, Tarrytown, N. Y., 1967.

Hewlett, J. D., and J. B. Moore, Predicting stormflow and peak discharges in the Redland District using the R-index method, *Rep. 84*, Ga. For. Res., Athens, 1976.

Hinton, M. J., S. L. Schiff, and M. C. English, Examining the contributions of glacial till water to storm runoff using two- and three-component hydrograph separation, *Water Resour. Res.*, *30*, 983–994, 1994.

Hooper, R. P., and C. A. Shoemaker, A comparison of chemical and isotopic hydrograph separation, *Water Resour. Res.*, *22*, 1444–1454, 1986.

Hooper, R. P., N. Christopherson, and N. E. Peters, Modelling streamwater chemistry as a mixture of soilwater end-members—An application to the Panola Mountain catchment, Georgia, USA, *J. Hydrol.*, *116*, 321–343, 1990.

Hornberger, G. M., T. M. Scanlon, and J. P. Raffensperger, Modelling transport of dissolved silica in a forested headwater catchment: The effect of hydrological and chemical time scales on hysteresis in the concentration-discharge relationship, *Hydrol. Processes*, *15*, 2029–2038, 2001.

Horton, R. E., The role of infiltration in the hydrologic cycle, *Eos Trans. AGU*, *14*, 446–460, 1933.

Kendall, C., J. J. McDonnell, and W. Gu, A look inside black box hydrograph separation models: A study at the Hydrohill catchment, *Hydrol. Processes*, *15*, 1877–1902, 2001.

Kennedy, V. C., C. Kendall, G. W. Zellweger, T. A. Wyerman, and R. J. Avanzino, Determination of the components of stormflow using water chemistry and environmental isotopes, Mattole River basin, California, *J. Hydrol.*, *84*, 107–140, 1986.

Kirby, M. J., and R. J. Chorley, Throughflow, overland flow, and erosion, *Bull. IAHS*, *12*, 5–21, 1967.

Leavesley, G. H., and L. G. Stannard, The precipitation- runoff modeling system—PRMS, in *Computer Models of Watershed Hydrology*, edited by V. P. Singh, pp. 281–310, Water Resour. Publ., Highlands Ranch, Colo., 1995.

McDonnell, J. J., A rationale for old water discharge through macropores in a steep, humid catchment, *Water Resour. Res.*, *26*, 2821–2832, 1990.

McDonnell, J. J., M. Bonell, M. K. Stewart, and A. J. Pearce, Deuterium variations in storm rainfall: Implications for stream hydrograph separations, *Water Resour. Res.*, *26*, 455–458, 1990.

McDonnell, J. J., D. D. Brammer, C. Kendall, N. Hjerdt, L. K. Rowe, M. Stewart, and R. A. Woods, Flow pathways on steep forested hillslopes: The tracer, tensiometer, and trough approach, in *Environmental Forest Science*, edited by M. Tani, pp. 463–474, Kluwer Acad., Norwell, Mass., 1998.

McGlynn, B. L., and J. J. McDonnell, Role of discrete landscape units in controlling catchment dissolved organic carbon dynamics, *Water Resour. Res.*, *39*(4), 1090, doi:10.1029/2002WR001525, 2003.

McGlynn, B. L., and J. Seibert, Distributed assessment of contributing area and riparian buffering along stream networks, *Water Resour. Res.*, *39*(4), 1082, doi:10.1029/2002WR001521, 2003.

McGlynn, B. L., J. J. McDonnell, J. B. Shanley, and C. Kendall, Riparian zone flowpath dynamics during snowmelt in a small headwater catchment, *J. Hydrol.*, *222*, 75–92, 1999.

McGlynn, B. L., J. J. McDonnell, and D. D. Brammer, A review of the evolving perceptual model of hillslope flowpaths at the Maimai catchments, New Zealand, *J. Hydrol.*, *257*, 1–26, 2002.

Moore, T. R., Dynamics of dissolved organic carbon in forested and disturbed catchments, Westland, New Zealand: 1. Maimai, *Water Resour. Res.*, *25*, 1321–1330, 1989.

Mosley, M. P., Streamflow generation in a forested watershed, New Zealand, *Water Resour. Res.*, *15*, 795–806, 1979.

Mosley, M. P., Subsurface flow velocities through selected forest soils, South Island, New Zealand, *J. Hydrol.*, *55*, 65–92, 1982.

Ogunkoya, O. O., and A. K. Jenkins, Analysis of storm hydrograph and flow pathways using a three-component hydrograph separation model, *J. Hydrol.*, *142*, 71–88, 1993.

O'Loughlin, C. L., L. K. Rowe, and A. J. Pearce, Sediment yields from small forested catchments, North Westland-Nelson, New Zealand, *N. Z. J. Hydrol.*, *17*, 1–15, 1978.

Pearce, A. J., and A. I. McKerchar, Upstream generation of storm runoff, in *Physical Hydrology: The New Zealand Experience*, edited by D. L. Murray and P. Ackroyd, pp. 165–192, N. Z. Hydrol. Soc., Wellington, 1979.

Pearce, A. J., and L. K. Rowe, Forest management effects on interception, evaporation and water yield, *N. Z. J. Hydrol.*, *18*, 73–87, 1979.

Pearce, A. J., C. L. O'Loughlin, and L. K. Rowe, Hydrologic regime of small undisturbed beech forest catchments, North Westland, in *Proceedings of the Third Soil and Plant Water Symposium*, *Publ. 1-126*, pp. 150–158, N. Z. Dep. of Sci. and Indust. Res., Lower Hutt, N. Z., 1976.

Pearce, A. J., M. K. Stewart, and M. G. Sklash, Storm runoff generation in humid headwater catchments: 1. Where does the water come from?, *Water Resour. Res.*, *22*, 1263–1272, 1986.

Pinder, G. F., and J. F. Jones, Determination of the ground-water component of peak discharge from the chemistry of total runoff, *Water Resour. Res.*, *5*, 438–445, 1969.

Ragan, R. M., An experimental investigation of partial area contributions, in *Proceedings of Symposium of Berne*, *Int. Assoc. Sci. Hydrol.*, *76*, 241–249, 1968.

Rice, K. C., and G. M. Hornberger, Comparison of hydrochemical tracers to estimate source contributions to peak flow in a small, forested, headwater catchment, *Water Resour. Res.*, *34*, 1755–1766, 1998.

Rodhe, A., The origin of streamwater traced by oxygen-18, Ph.D. dissertation, Uppsala Univ., Uppsala, Sweden, 1987.

Rowe, L. K., A. J. Pearce, and C. L. O'Loughlin, Hydrology and related changes after harvesting native forest catchments and establishing Pinus radiata plantations, part 1, An introduction to the study, *Hydrol. Processes*, *8*, 263–279, 1994.

Scanlon, T. M., J. P. Raffensperger, and G. M. Hornberger, Modeling transport of dissolved silica in a forested headwater catchment: Implications for defining the hydrochemical response of observed flow pathways, *Water Resour. Res.*, *37*, 1071–1082, 2001.

Sidle, R. C., Y. Tsuboyama, S. Noguchi, I. Hosoda, M. Fujieda, and T. Shimizu, Stormflow generation in steep forested headwaters: A linked hydrogeomorphic paradigm, *Hydrol. Processes*, *14*, 369–385, 2000.

Sklash, M. G., M. K. Stewart, and A. J. Pearce, Storm runoff generation in humid headwater catchments: 2. A case study of hillslope and low-order stream response, *Water Resour. Res.*, *22*, 1273–1282, 1986.

Uhlenbrook, S., Examination and modeling of the runoff generation in a mesoscale basin (in German), Ph.D. thesis, 193 pp., Inst. of Hydrol., Univ. of Freiburg, Freiburg, Germany, 1999.

Webster, J., The hydrologic properties of the forest floor under beech/podocarp/hardwood forest, North Westland, M.S. thesis, Univ. of Canterbury, Christchurch, N. Z., 1977.

Weyman, D. R., Throughflow on hillslopes and its relation to the stream hydrograph, *Bull. Int. Assoc. Sci. Hydrol.*, *15*, 25–33, 1970.

Whipkey, R. Z., Subsurface storm flow from forested slopes, *Bull. Int. Assoc. Sci. Hydrol.*, *2*, 74–85, 1965.

Wigmosta, M. S., L. W. Vail, and D. P. Lettenmaier, A distributed hydrology-vegetation model for complex terrain, *Water Resour. Res.*, *30*, 1665–1679, 1994.

Woods, R. A., and L. K. Rowe, The changing spatial variability of subsurface flow across a hillside, *N. Z. J. Hydrol.*, *35*, 51–86, 1996.

Woods, R. A., M. Sivapalan, and J. S. Robinson, Modeling the spatial variability of subsurface runoff using a topographic index, *Water Resour. Res.*, *33*, 1061–1073, 1997.

J. J. McDonnell, Department of Forest Engineering, Oregon State University, Corvallis, OR 97331-5706, USA. (jeffrey.mcdonnell@orst.edu)

B. L. McGlynn, Department of Land Resources and Environmental Sciences, Montana State University, 334 Leon Johnson Hall, P.O. Box 173120, Bozeman, MT 59717, USA. (bmcglynn@montana.edu)